Modeling star formation today and in the early universe

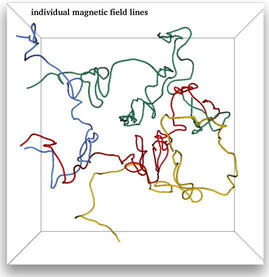


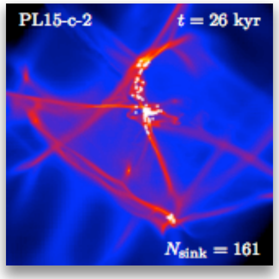

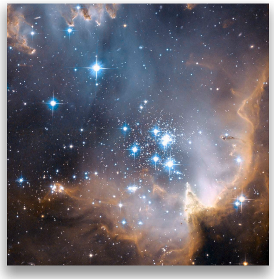
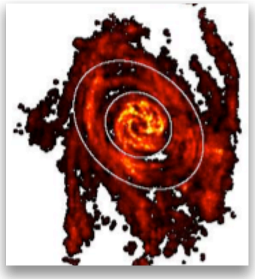
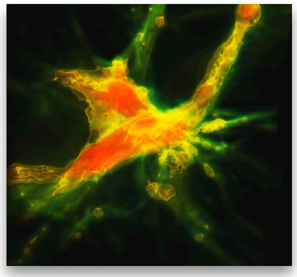

Ralf Klessen

Zentrum für Astronomie der Universität Heidelberg
Institut für Theoretische Astrophysik

thanks

- to the organizers to bring us to this very nice place

NGC 3324 (Hubble, NASA/ESA)

thanks

- to the organizers to bring us to this very nice place
- thanks also to many collaborators

  ... people in the group in Heidelberg:
  Richard Allison, Gabriel Anorve, Christian Baczynski, Erik Bertram, Frank Bigiel, Paul Clark, Gustavo Dopcke, Jayanta Dutta, Philipp Girichidis, Simon Glover, Lukas Konstandin, Faviola Molina, Milica Micic, Mei Sasaki, Jennifer Schober, Rahul Shetty, Rowan Smith

  ... former group members:
  Robi Banerjee, Ingo Berentzen, Christoph, Federrath, Thomas Greif, Thomas Peters, Dominik Schleicher, Sharanya Sur

NGC 3324 (Hubble, NASA/ESA)

agenda

- some phenomenology
- some aspects of star formation
  - thermodynamics
  - gravoturbulent fragmentation vs. disk fragmentation
- TreeCol

NGC 3324 (Hubble, NASA/ESA)


Carina with HST

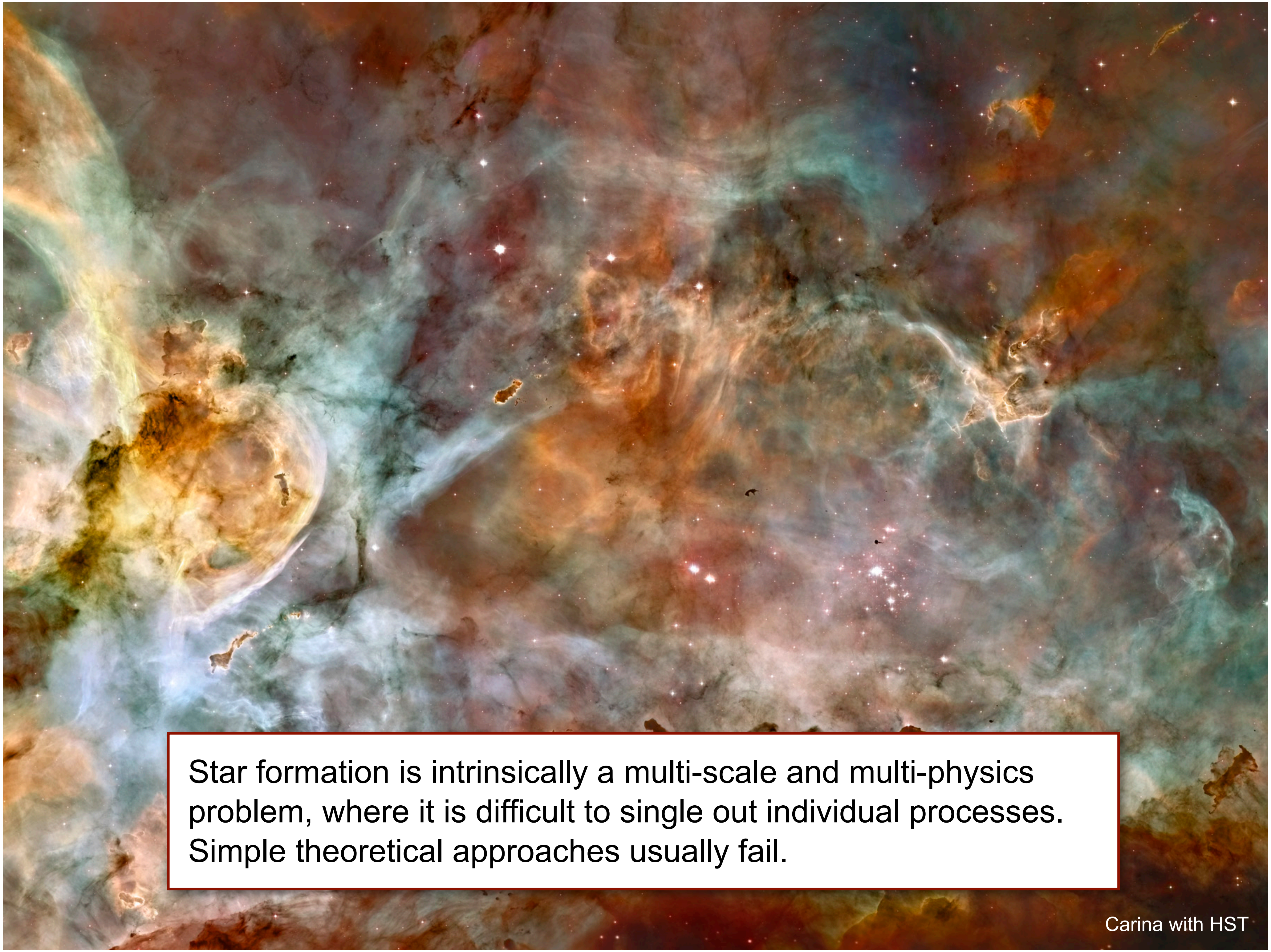

Star formation is intrinsically a multi-scale and multi-physics problem, where it is difficult to single out individual processes. Simple theoretical approaches usually fail.

Carina with HST

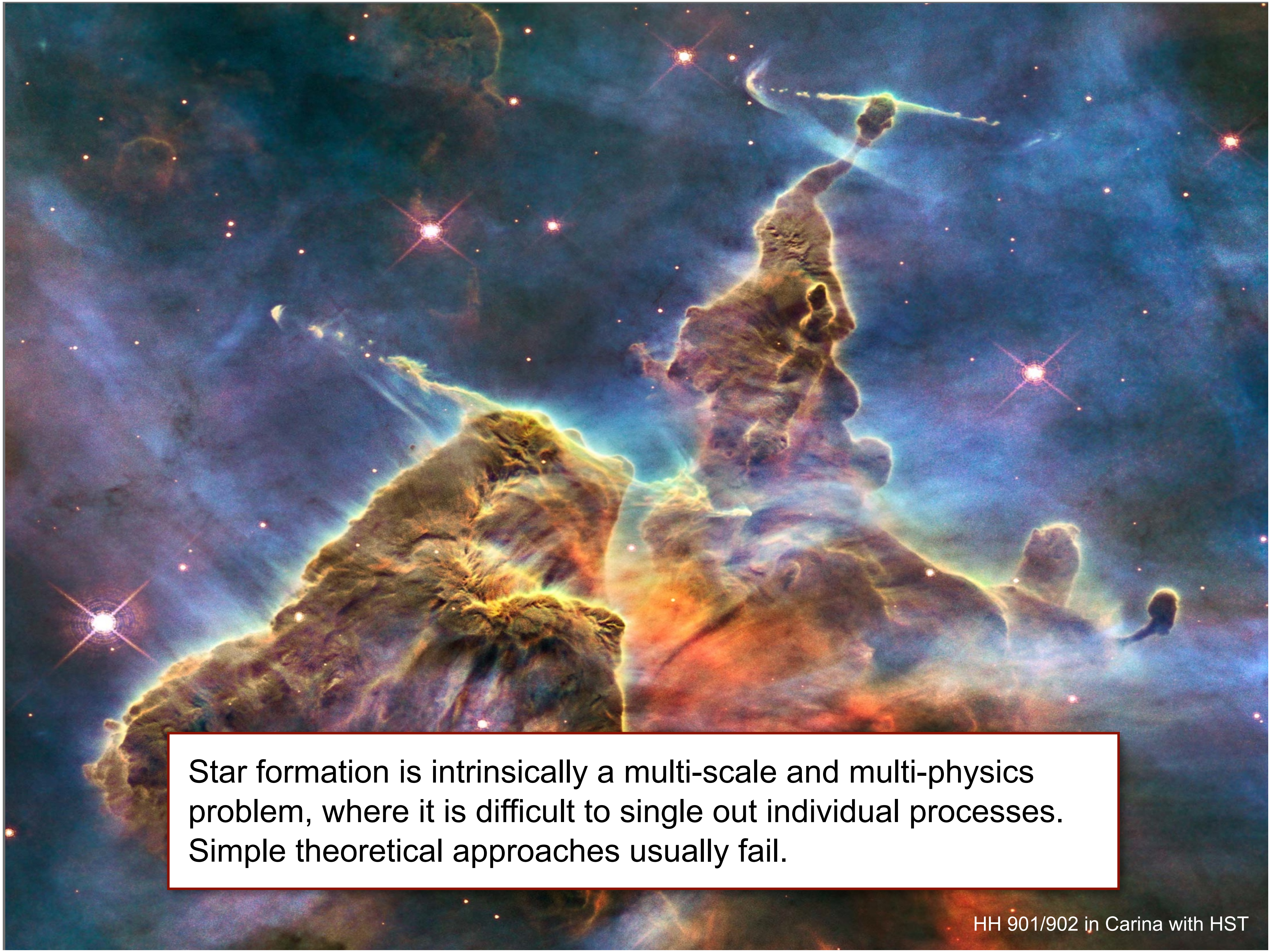

Star formation is intrinsically a multi-scale and multi-physics problem, where it is difficult to single out individual processes. Simple theoretical approaches usually fail.

HH 901/902 in Carina with HST

Stellar mass function

stellar mass fuction

stars seem to follow a universal mass function at birth --> IMF

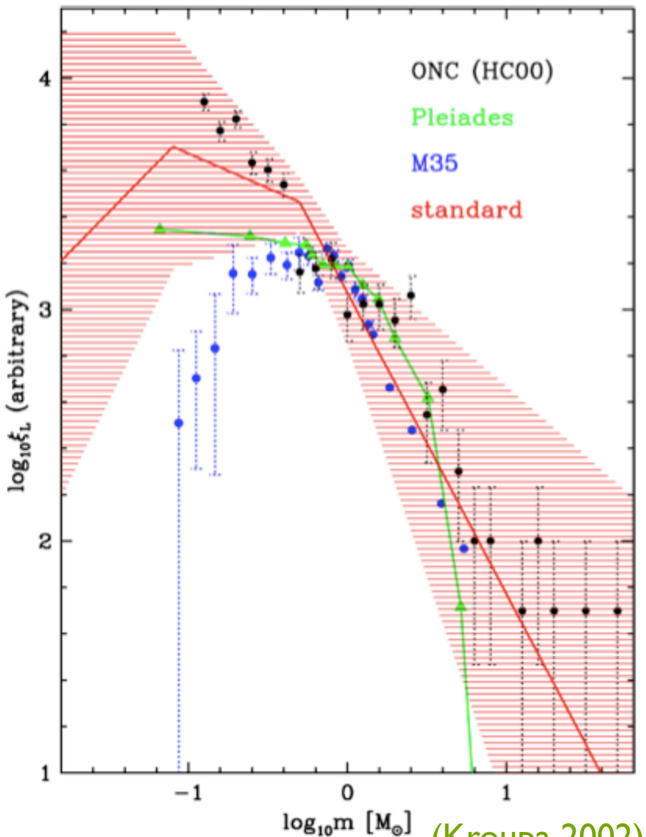

(Kroupa 2002)

Orion, NGC 3603, 30 Doradus
(Zinnecker & Yorke 2007)

stellar masses

- distribution of stellar masses depends on
  - turbulent initial conditions
    --> mass spectrum of prestellar cloud cores
  - collapse and interaction of prestellar cores
    --> accretion and *N*-body effects
  - thermodynamic properties of gas
    --> balance between heating and cooling
    --> EOS (determines which cores go into collapse)
  - (proto) stellar feedback terminates star formation
    ionizing radiation, bipolar outflows, winds, SN

(Kroupa 2002)

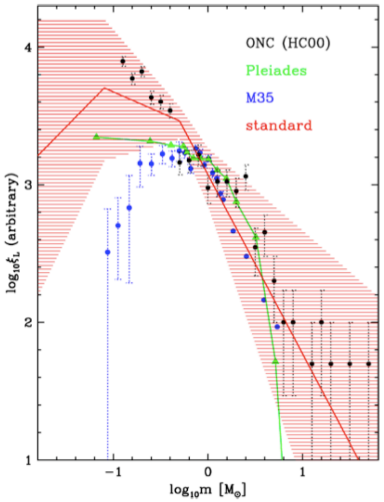

stellar masses

- distribution of stellar masses depends on
  - turbulent initial conditions
    --> mass spectrum of prestellar cloud cores
  - collapse and interaction of prestellar cores
    --> accretion and *N*-body effects
  - thermodynamic properties of gas
    --> balance between heating and cooling
    --> EOS (determines which cores go into collapse)
  - (proto) stellar feedback terminates star formation
    ionizing radiation, bipolar outflows, winds, SN

(Kroupa 2002)

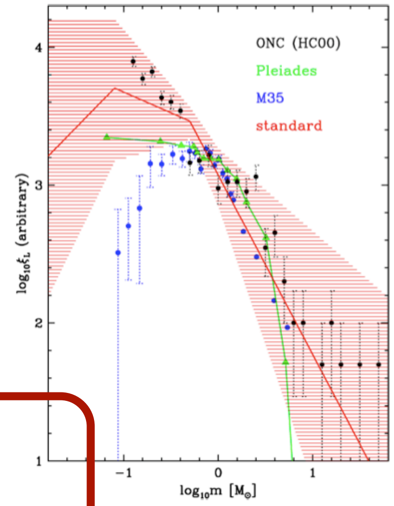

application to early star formation

thermodynamics & fragmentation

degree of fragmentation depends on *EOS!*

polytropic EOS: $\mathbf{p} \propto \rho^{\gamma}$

$\gamma<1$: dense cluster of low-mass stars

$\gamma>1$: isolated high-mass stars

(see Li et al. 2003; also Kawachi & Hanawa 1998, Larson 2003)

dependency on EOS

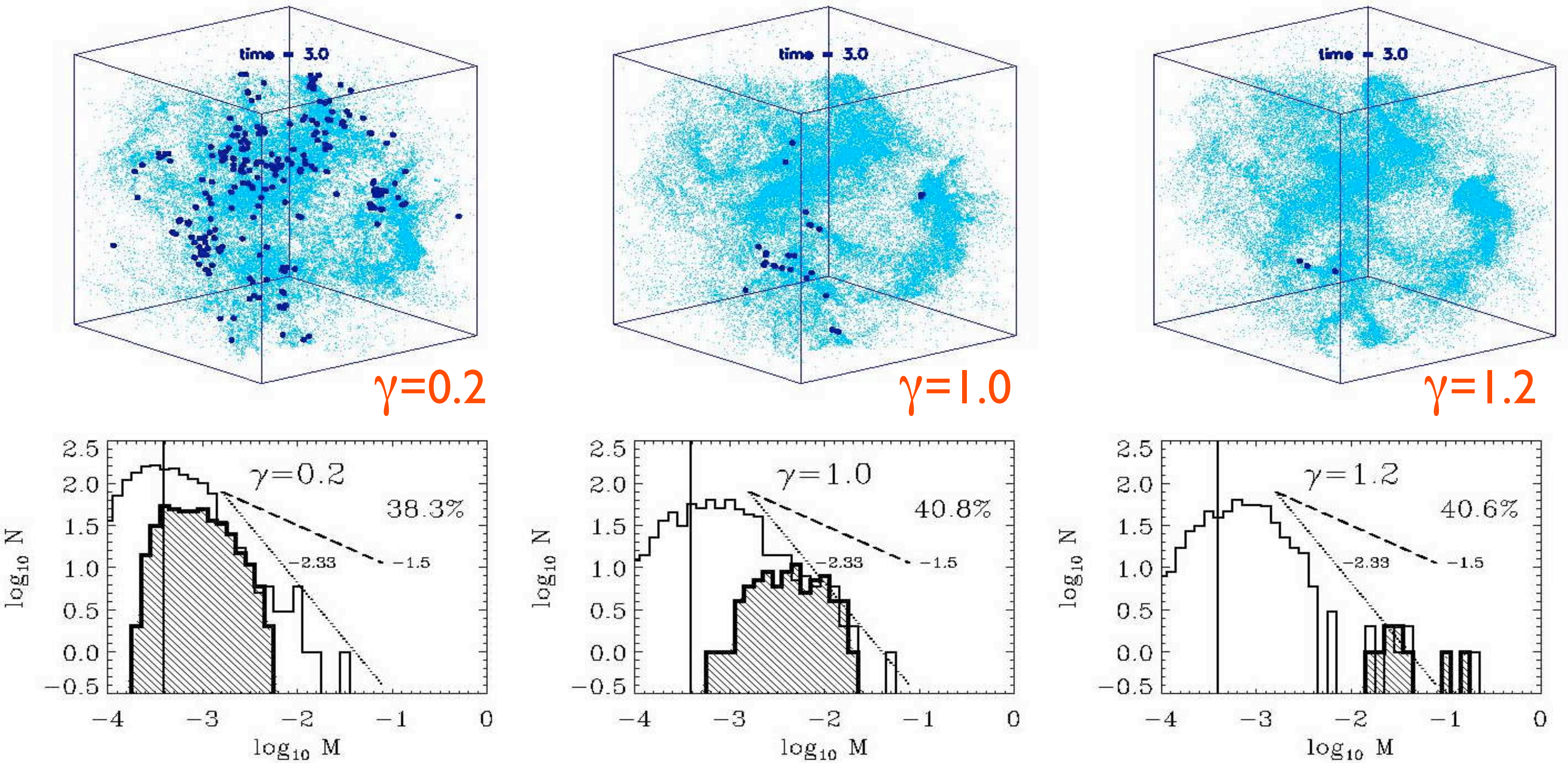

for $\gamma<1$ fragmentation is enhanced → *cluster of low-mass stars*

for $\gamma>1$ it is suppressed → formation of *isolated massive stars*

(from Li, Klessen, & Mac Low 2003, ApJ, 592, 975)

how does that work?

(1) $\mathbf{p} \propto \rho^{\gamma} \quad \rightarrow \quad \rho \propto \mathbf{p}^{1/\gamma}$

(2) $\mathbf{M_{jeans}} \propto \gamma^{3/2} \rho^{(3\gamma-4)/2}$

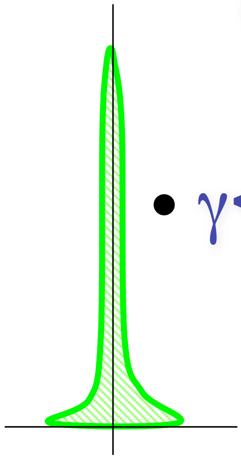

- $\gamma<1$: → *large* density excursion for given pressure
  → $\langle M_{jeans} \rangle$ becomes small
  → number of fluctuations with $M > M_{jeans}$ is large

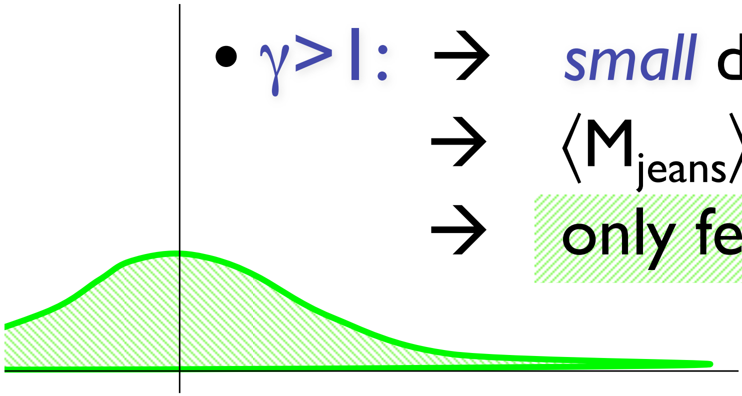

- $\gamma>1$: → *small* density excursion for given pressure
  → $\langle M_{jeans} \rangle$ is large
  → only few and massive clumps exceed M_{jeans}

EOS as function of metallicity

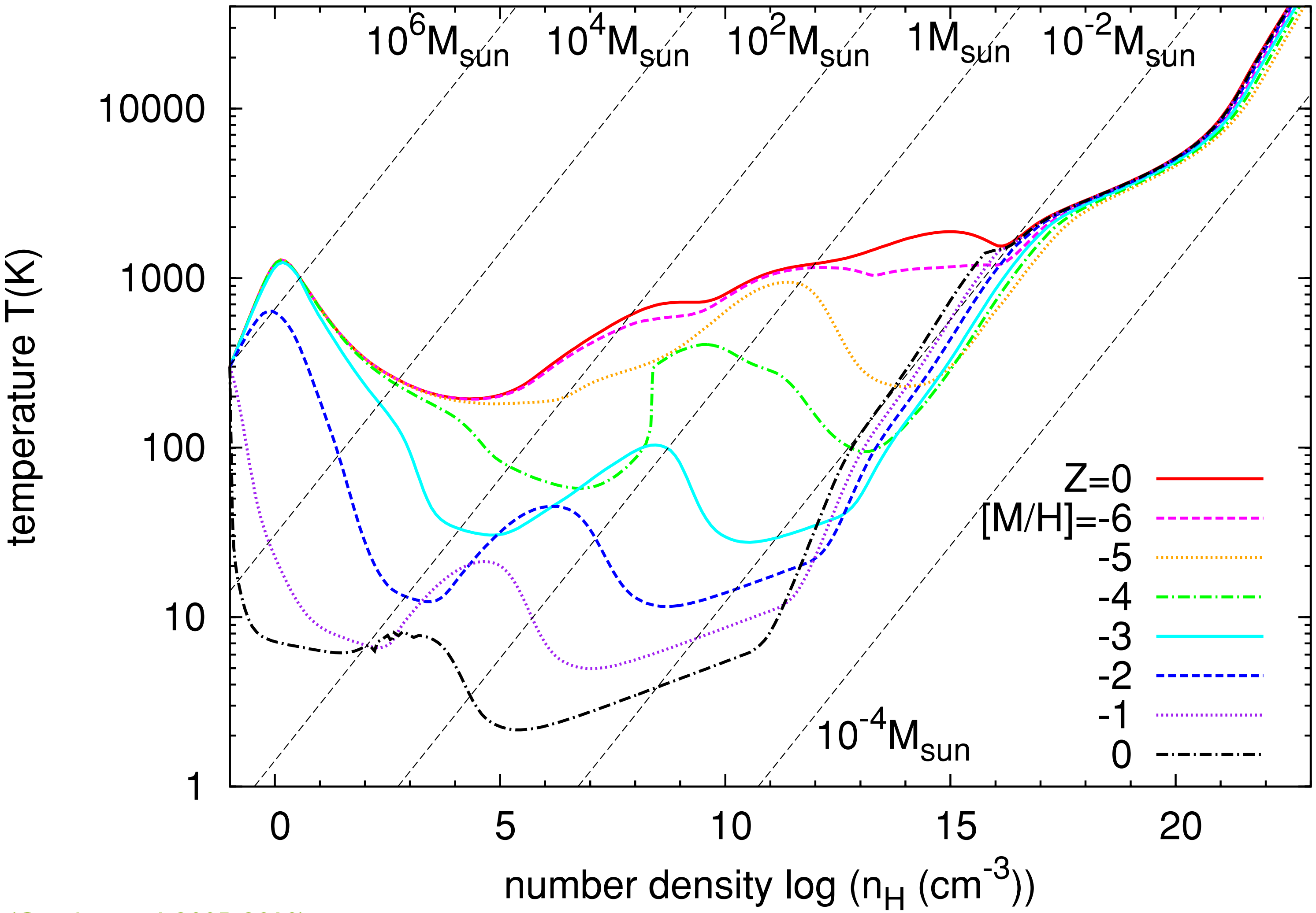

(Omukai et al. 2005, 2010)

EOS as function of metallicity

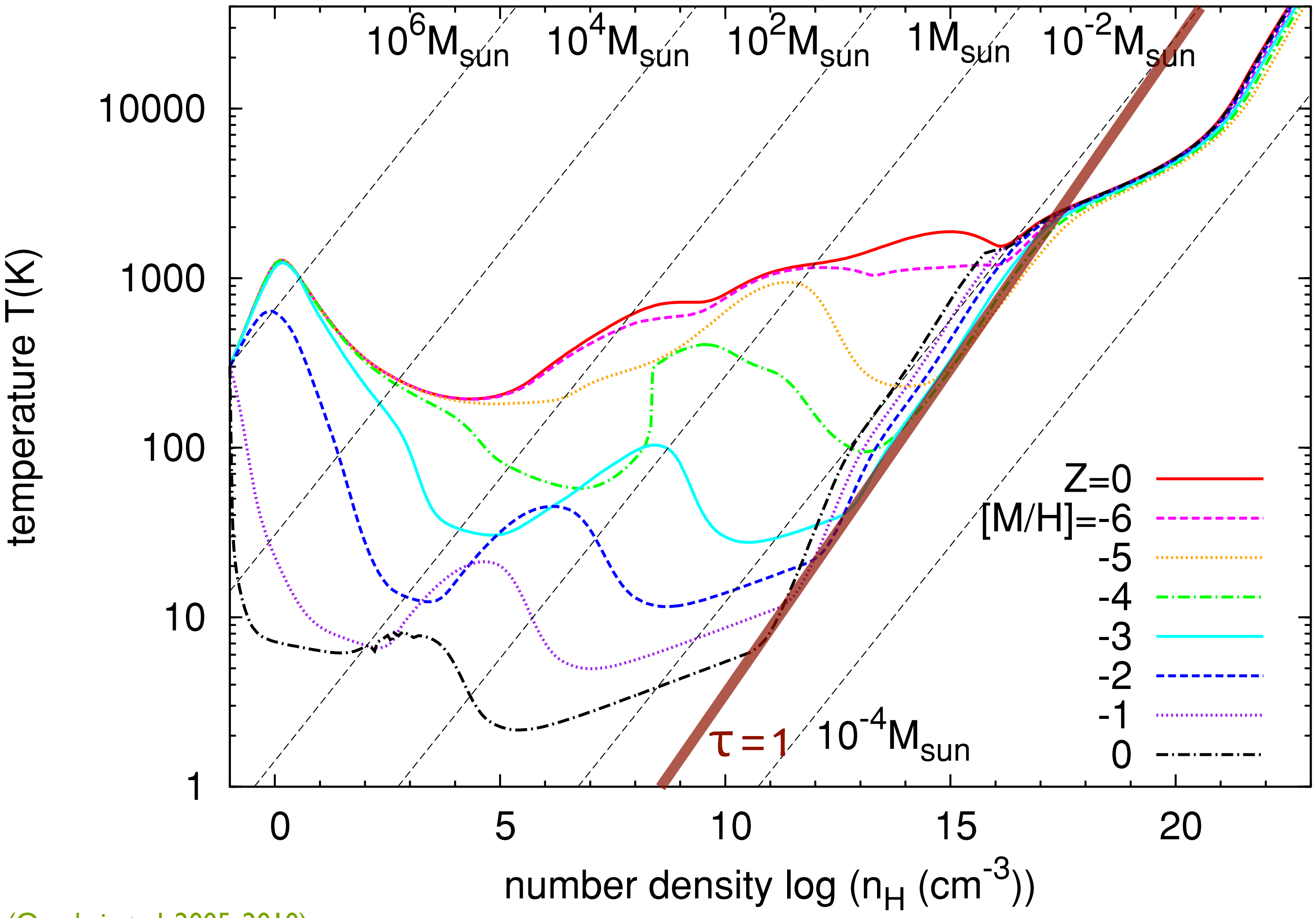

(Omukai et al. 2005, 2010)

EOS as function of metallicity

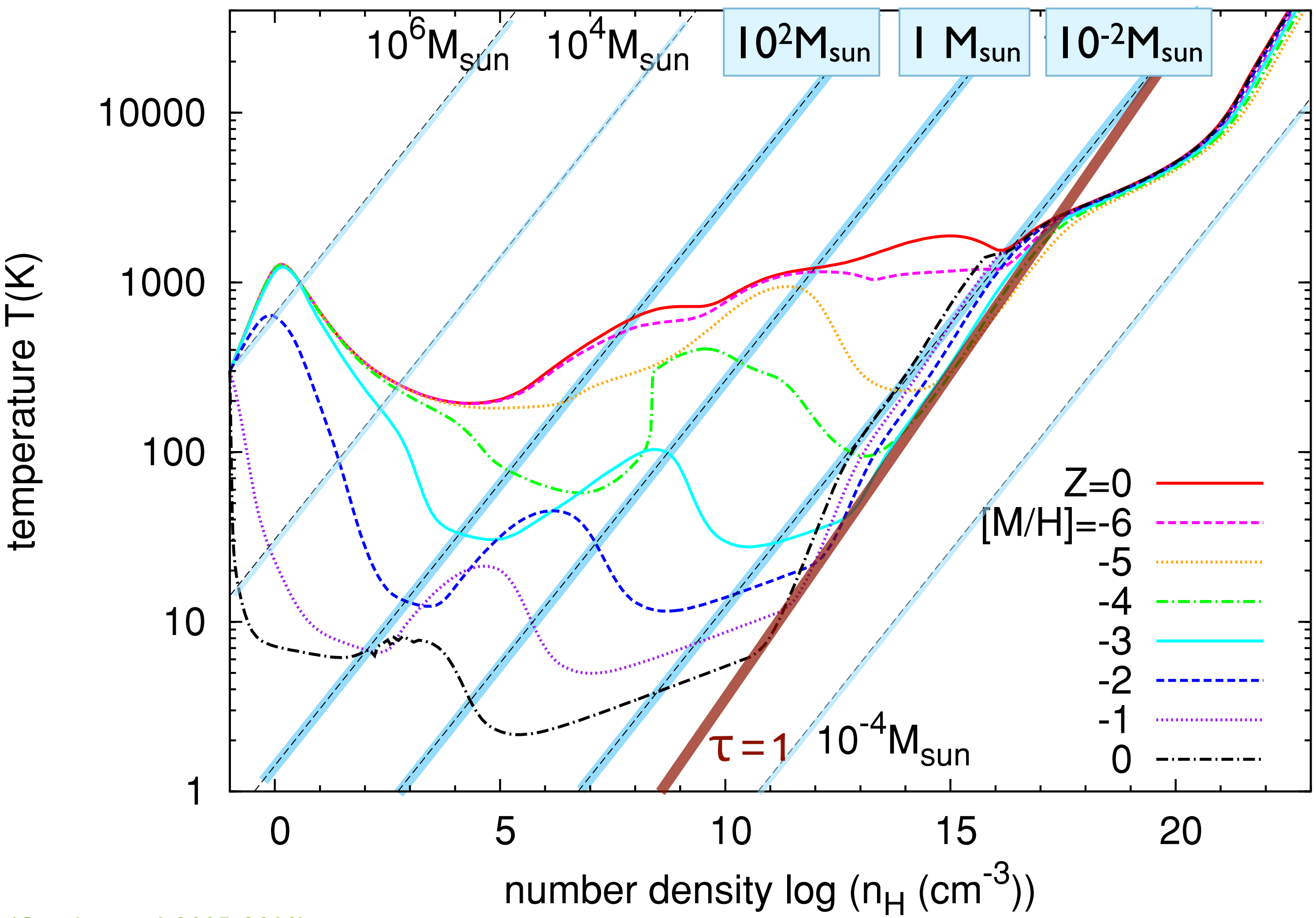

(Omukai et al. 2005, 2010)

EOS as function of metallicity

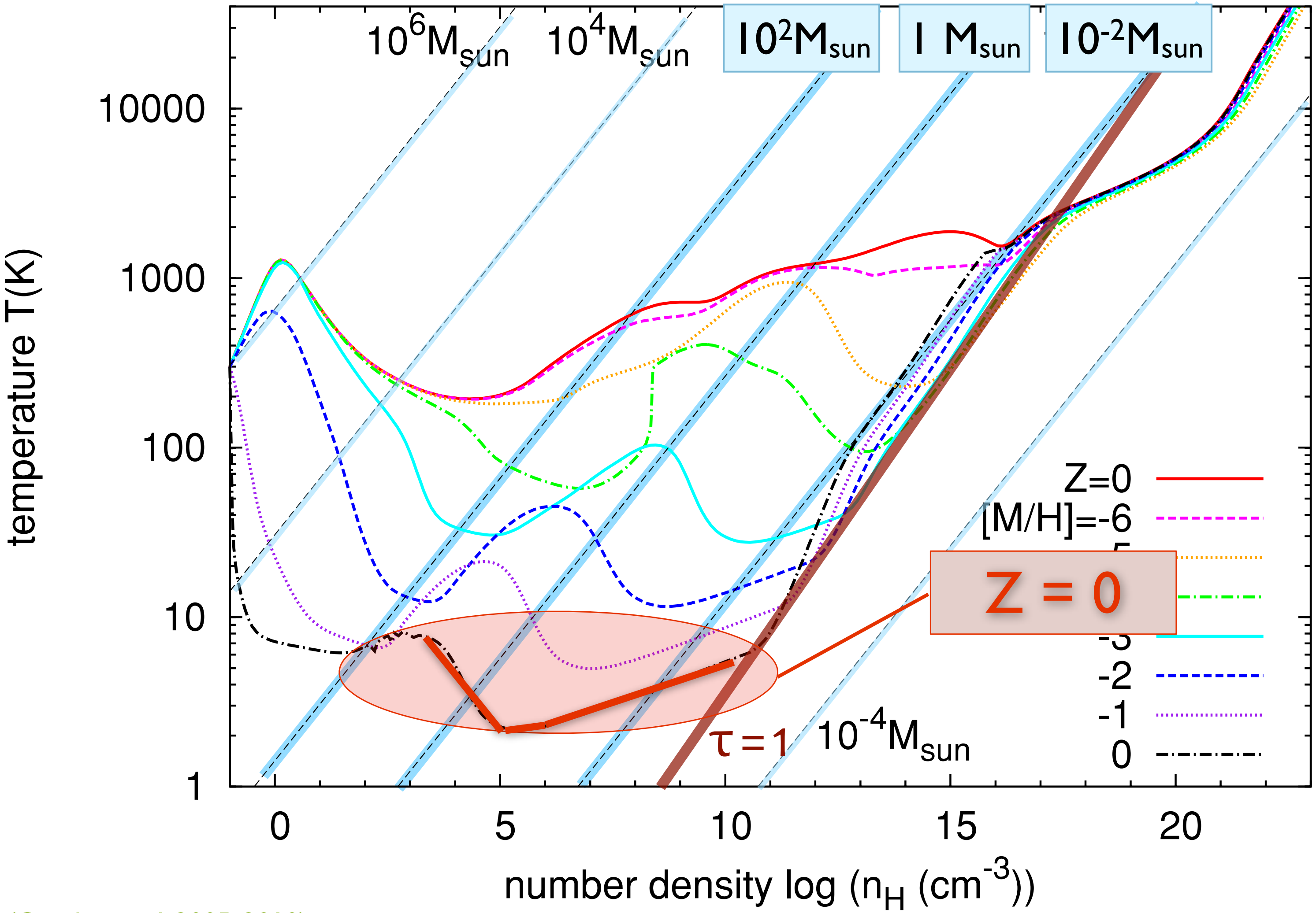

(Omukai et al. 2005, 2010)

present-day star formation

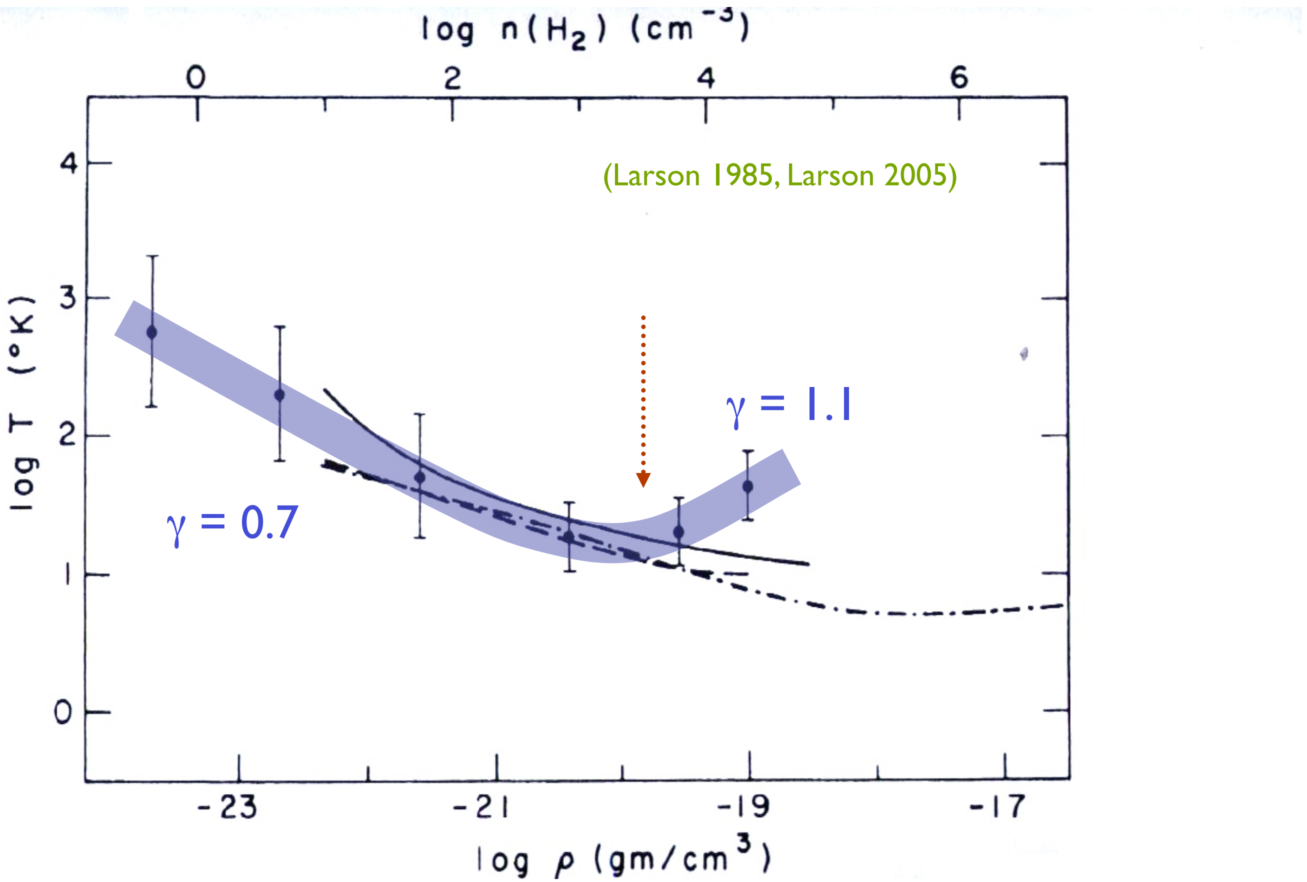

IMF in nearby molecular clouds

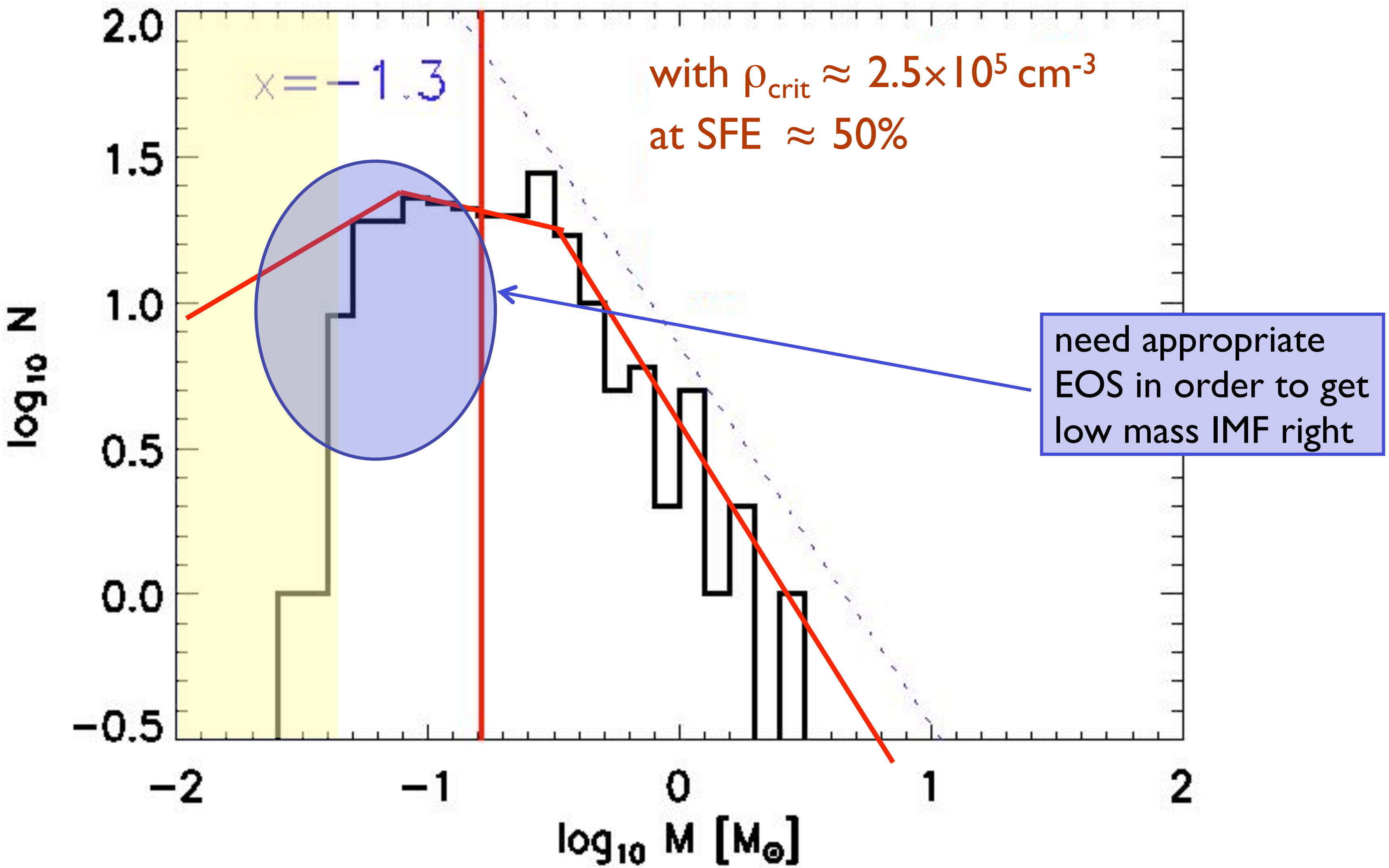

(Jappsen et al. 2005, A&A, 435, 611)

EOS as function of metallicity

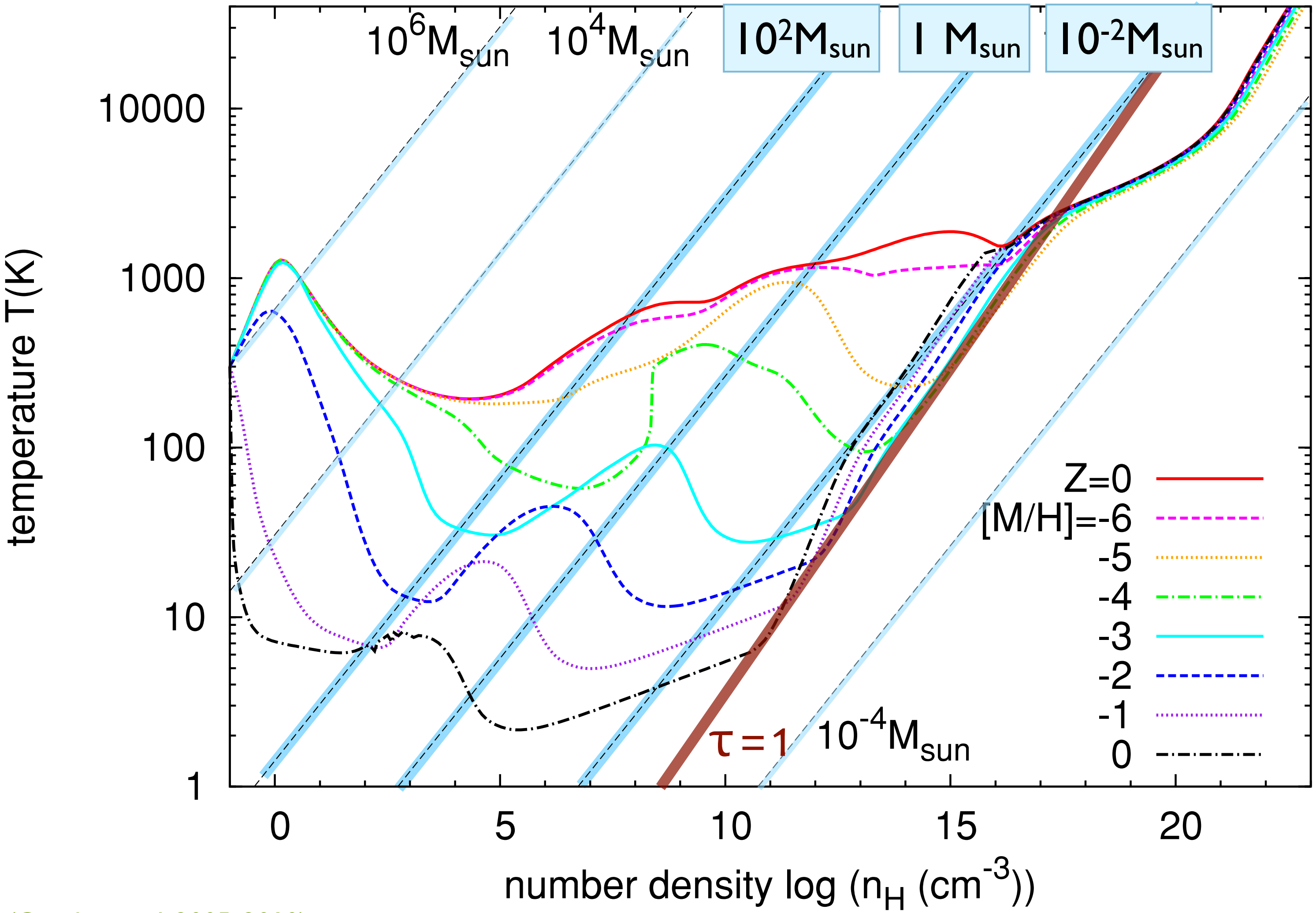

(Omukai et al. 2005, 2010)

EOS as function of metallicity

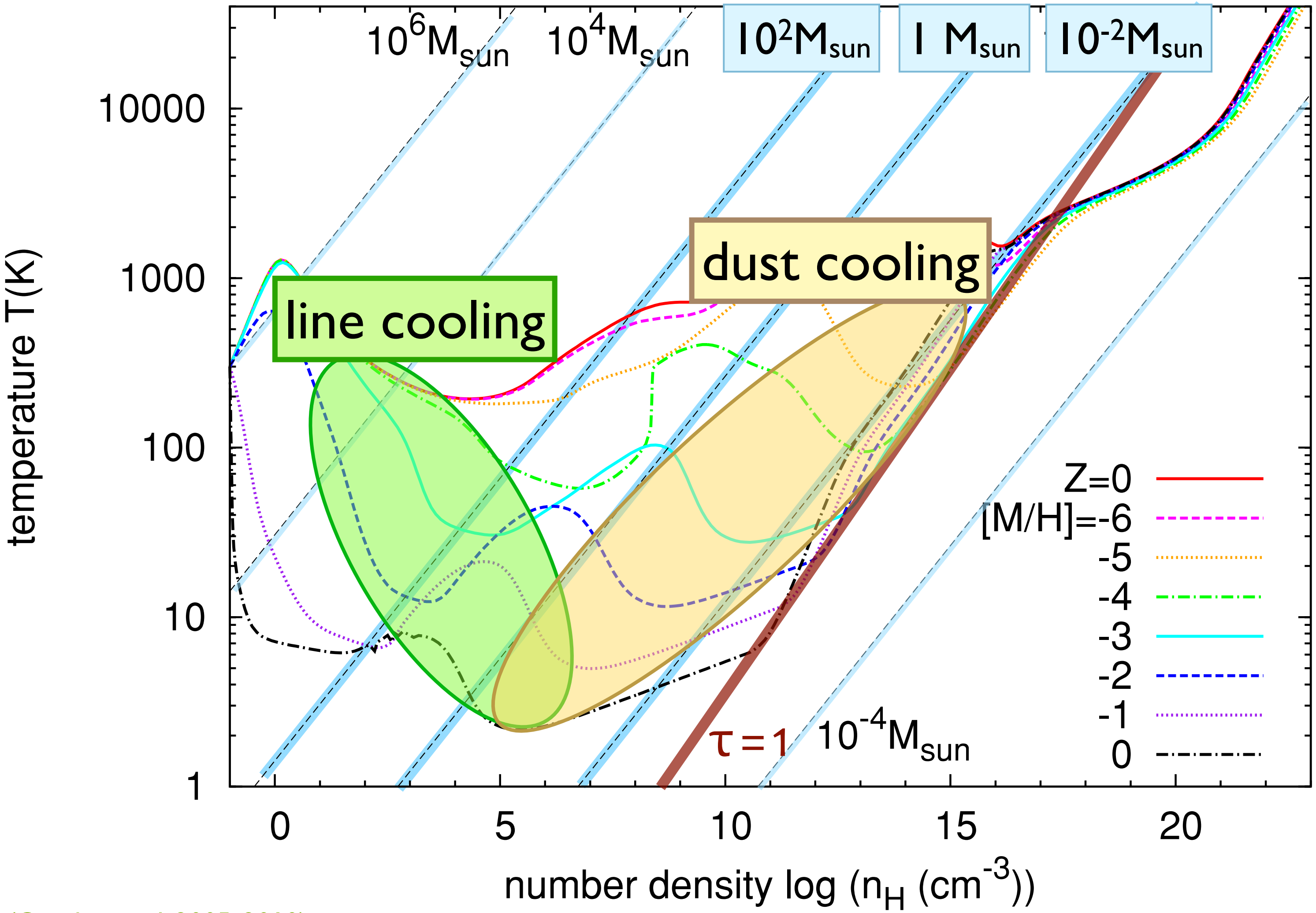

(Omukai et al. 2005, 2010)

transition: Pop III to Pop II.5

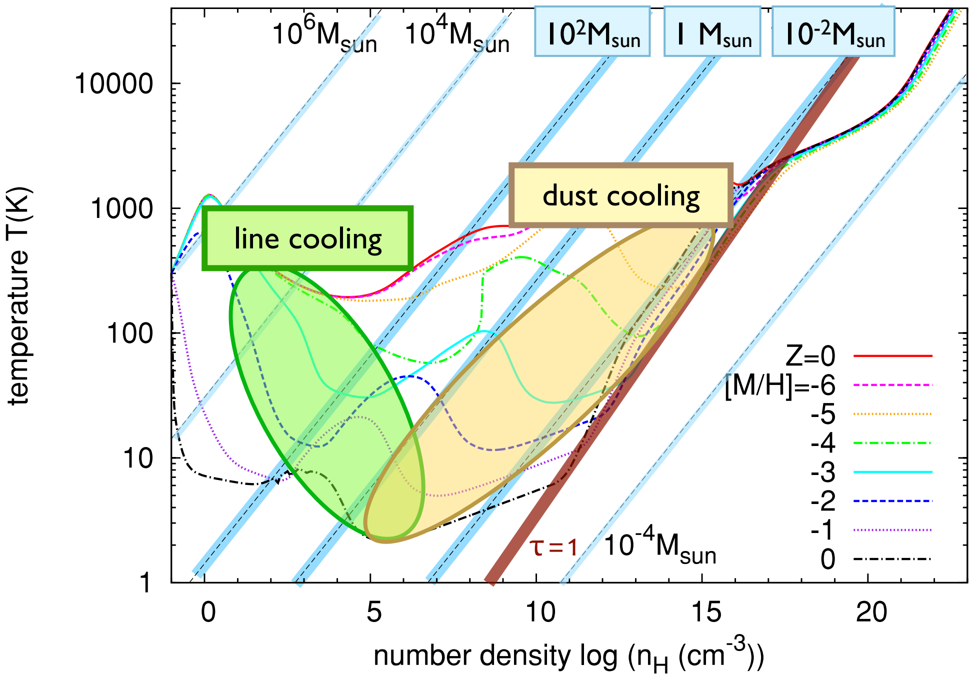

(Omukai et al. 2005, 2010)

two competing models:

- cooling due to atomic fine-structure lines ($Z > 10^{-3.5} Z_{sun}$)
- cooling due to coupling between gas and dust ($Z > 10^{-5...-6} Z_{sun}$)

- which one is explains origin of extremely metal-poor stars
  NB: lines would only make very massive stars, with $M >$ few x10 M_{sun}.

transition: Pop III to Pop II.5

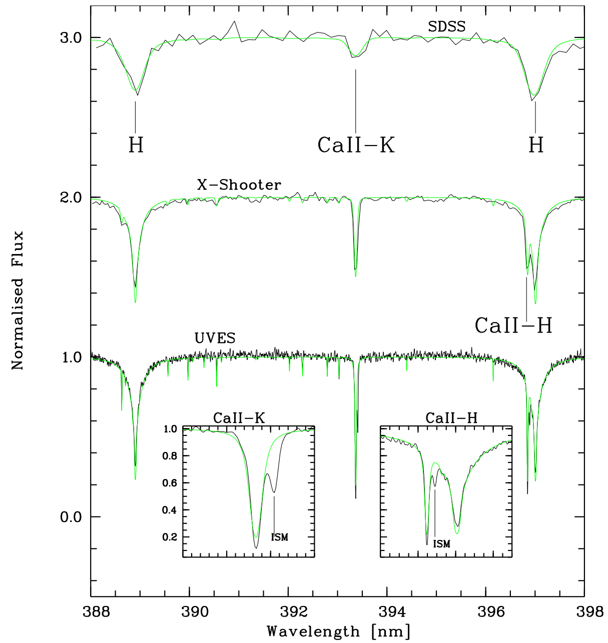

SDSS J1029151+172927

- is first ultra metal-poor star with Z ~ $10^{-4.5}$ Z_{sun} for all metals seen (Fe, C, N, etc.)
  [see Caffau et al. 2011]
- this is in regime, where metal-lines cannot provide cooling
- this star in Leo is incompatible with metal-line cooling!
  [see Schneider et al. 2011, Klessen et al. 2012]
- new ESO large program to find more of these stars (120h x-shooter, 30h UVES)

Element	$[X/H]_{1D}$	+3Dcor.	+NLTE cor.	+ 3D cor + NLTE cor	N lines	S_H	$A(X)_\odot$
C	≤ -3.8	≤ -4.5			G-band		8.50
N	≤ -4.1	≤ -5.0			NH-band		7.86
Mg I	-4.71 ± 0.11	-4.68 ± 0.11	-4.52 ± 0.11	-4.49 ± 0.12	5	0.1	7.54
Si I	-4.27	-4.30	-3.93	-3.96	1	0.1	7.52
Ca I	-4.72	-4.82	-4.44	-4.54	1	0.1	6.33
Ca II	-4.81 ± 0.11	-4.93 ± 0.03	-5.02 ± 0.02	-5.15 ± 0.09	3	0.1	6.33
Ti II	-4.75 ± 0.18	-4.83 ± 0.16	-4.76 ± 0.18	-4.84 ± 0.16	6	1.0	4.90
Fe I	-4.73 ± 0.13	-5.02 ± 0.10	-4.60 ± 0.13	-4.89 ± 0.10	43	1.0	7.52
Ni I	-4.55 ± 0.14	-4.90 ± 0.11			10		6.23
Sr II	≤ -5.10	≤ -5.25	≤ -4.94	≤ -5.09	1	0.01	2.92

(Caffau et al. 2011, 2012)

(Schneider et al. 2011, Klessen et al. 2012)

transition: Pop III to Pop II.5

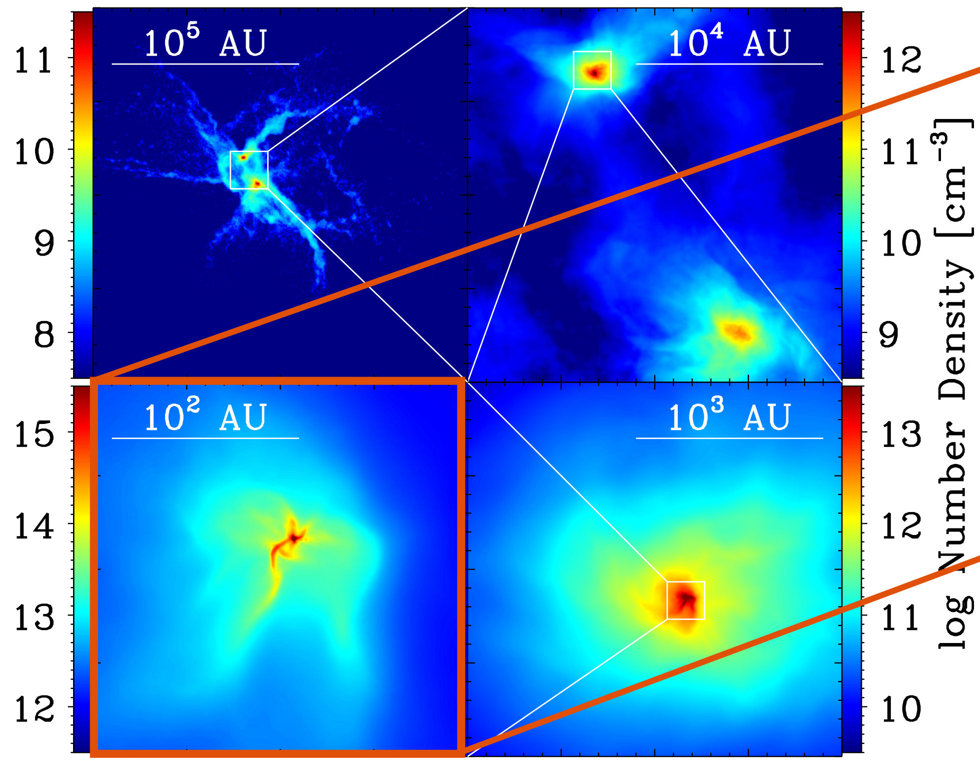

FIG. 2.— Number density maps for a slice through the high density region. The image shows a sequence of zooms in the density structure in the gas immediately before the formation of the first protostar.

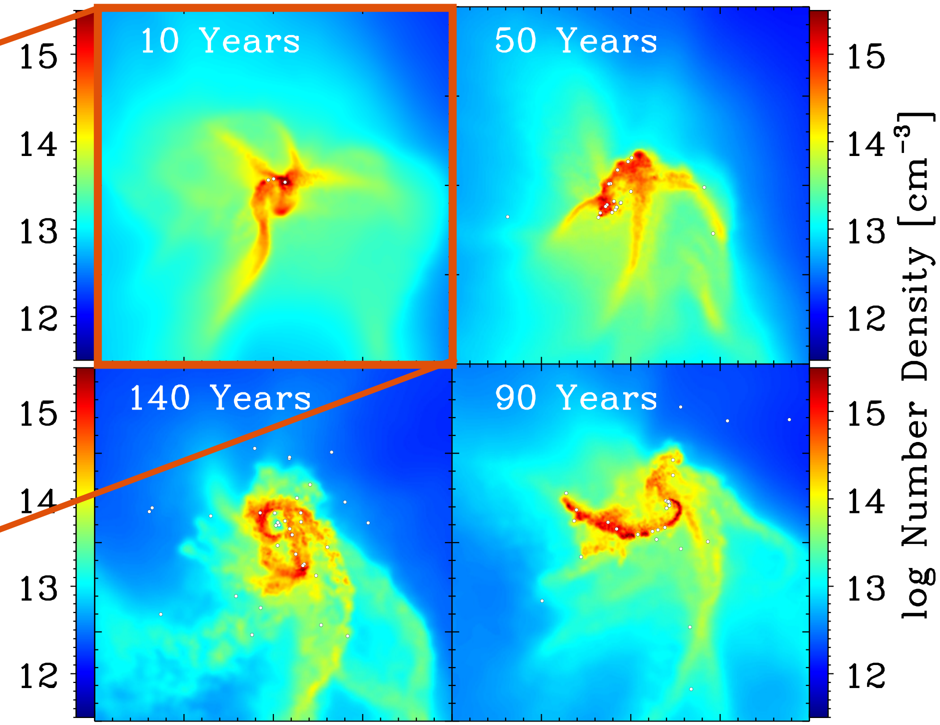

FIG. 3.— Number density map showing a slice in the densest clump, and the sink formation time evolution, for the 40 million particles simulation, and Z = $10^{-4} Z_{\odot}$. The box is 100AU x 100AU and the time is measured from the formation of the first sink particle.

Dopcke et al. (2011, ApJ 729, L3)

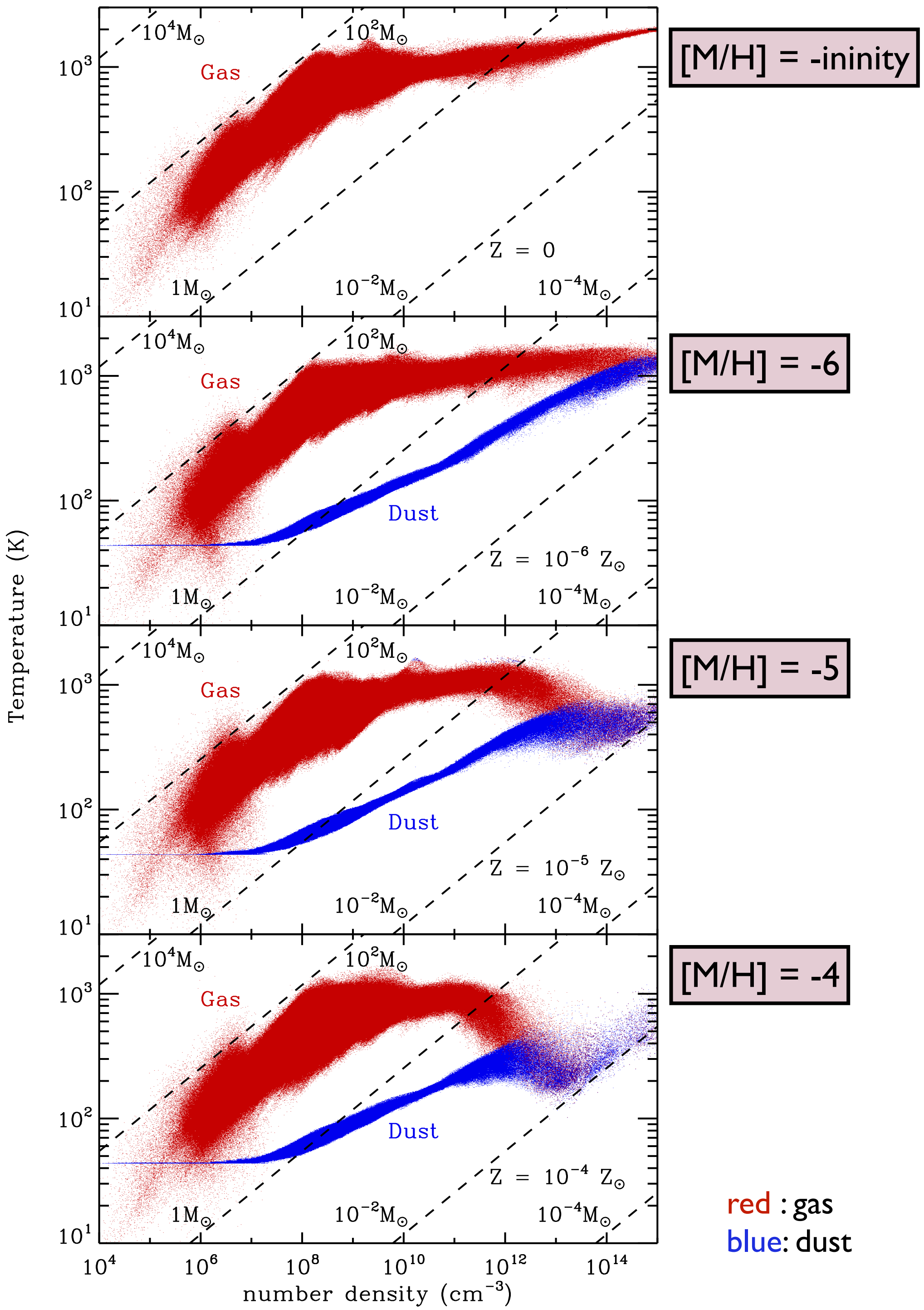

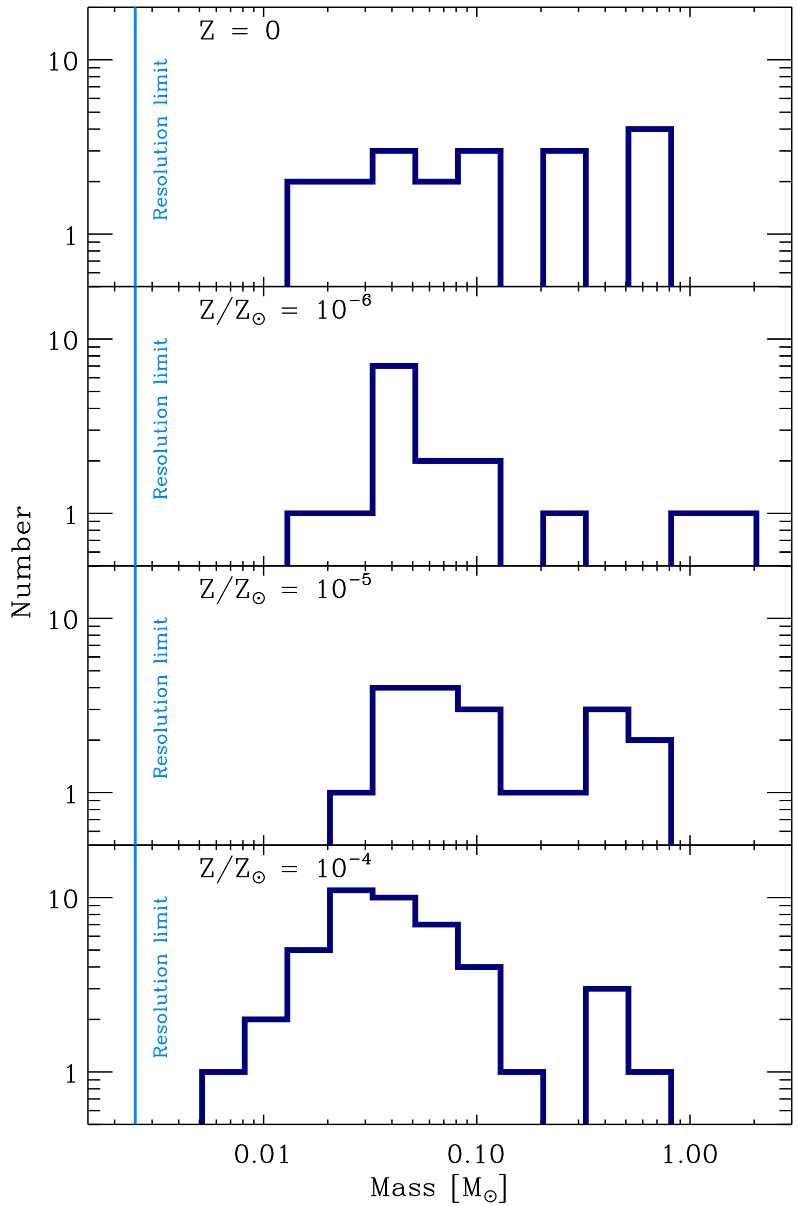

Dopcke et al., in prep.

disk fragmentation mode

gravoturbulent fragmentation mode

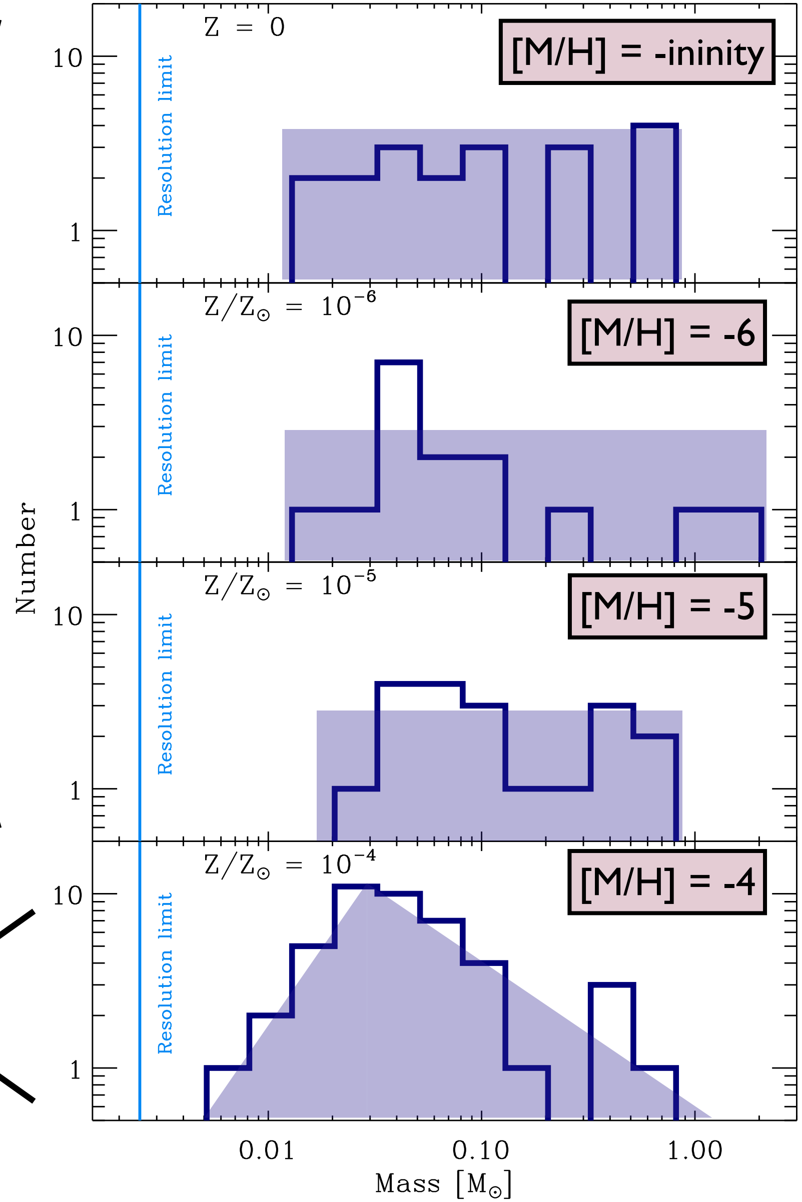

Dopcke et al., in prep.

EOS as function of metallicity

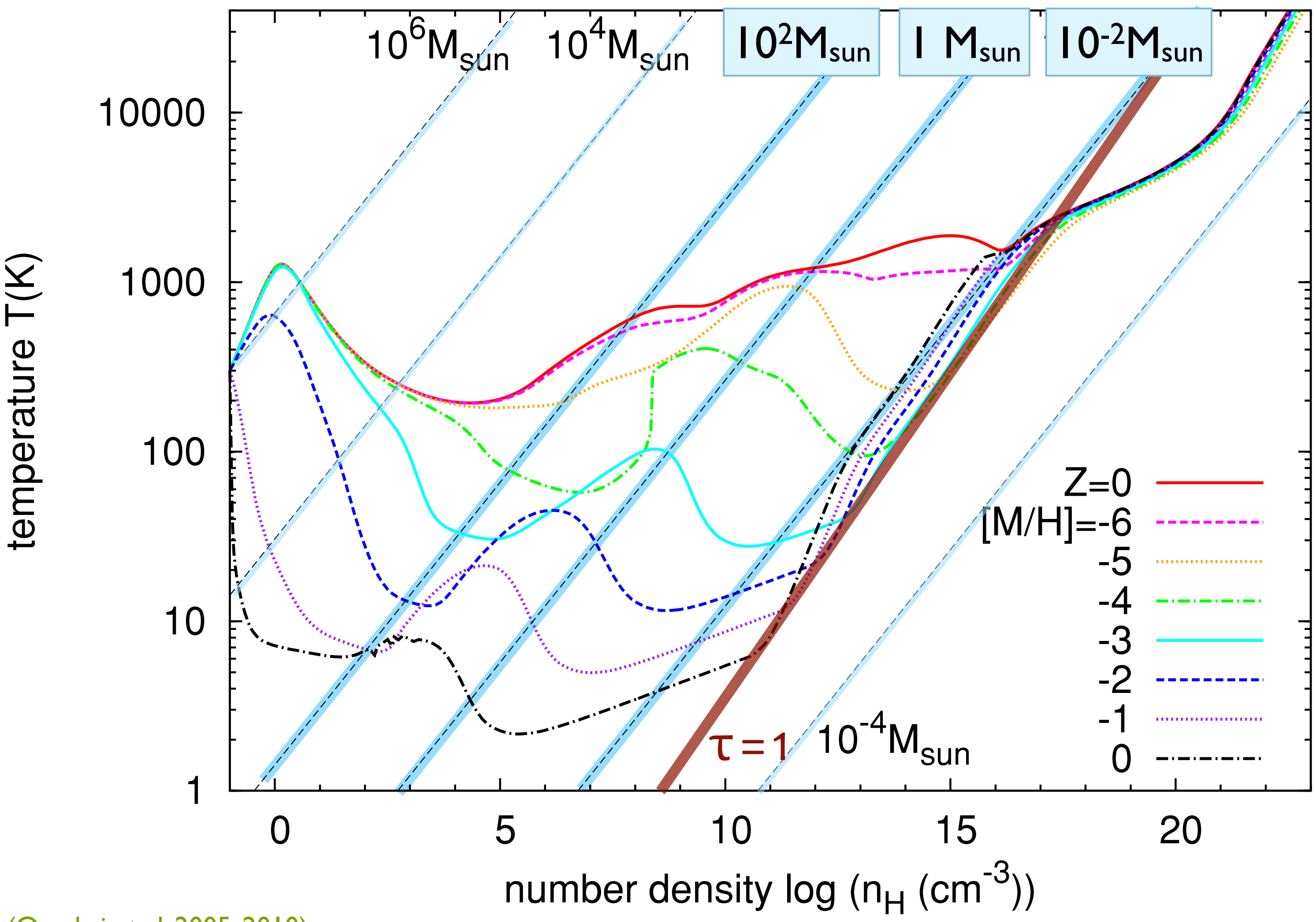

(Omukai et al. 2005, 2010)

EOS as function of metallicity

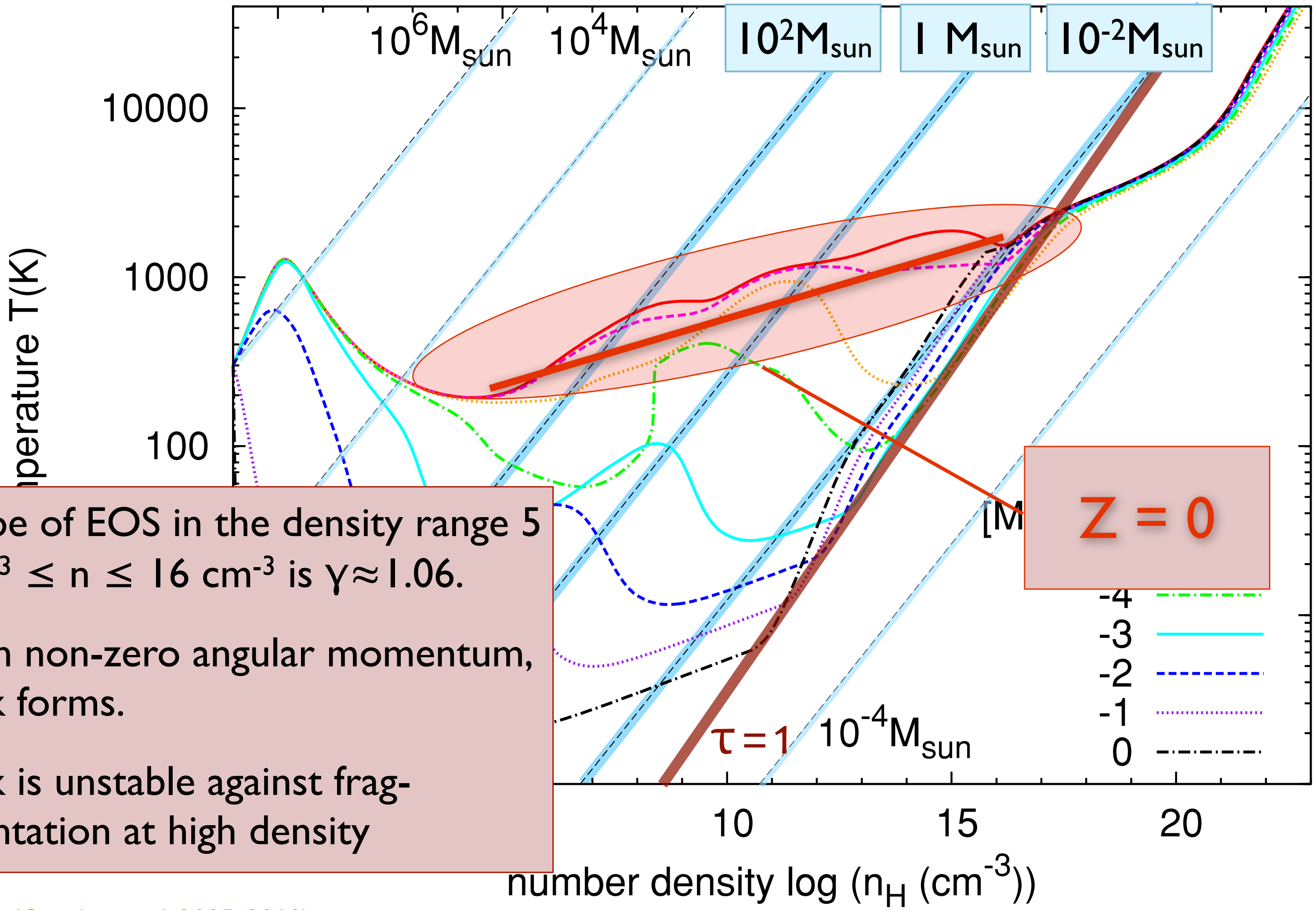

- slope of EOS in the density range 5 $cm^{-3} \leq n \leq 16\ cm^{-3}$ is $\gamma \approx 1.06$.
- with non-zero angular momentum, disk forms.
- disk is unstable against frag-mentation at high density

(Omukai et al. 2005, 2010)

detailed look at accretion disk around first star

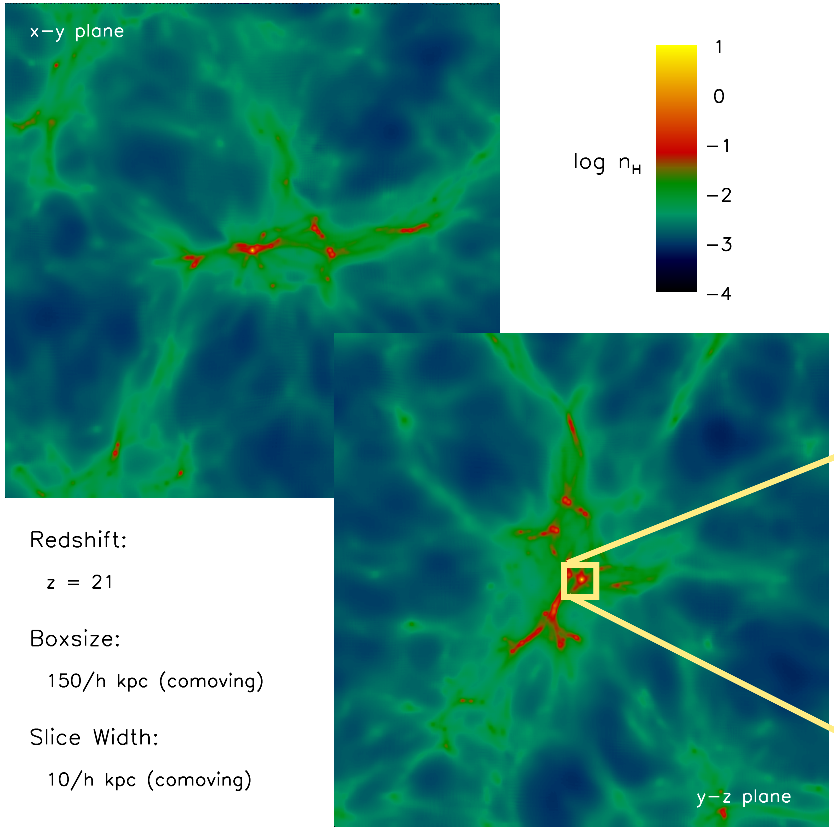

(Greif et al., 2007, ApJ, 670, 1)

successive zoom-in calculation from cosmological initial conditions (using SPH and new grid-code AREPO)

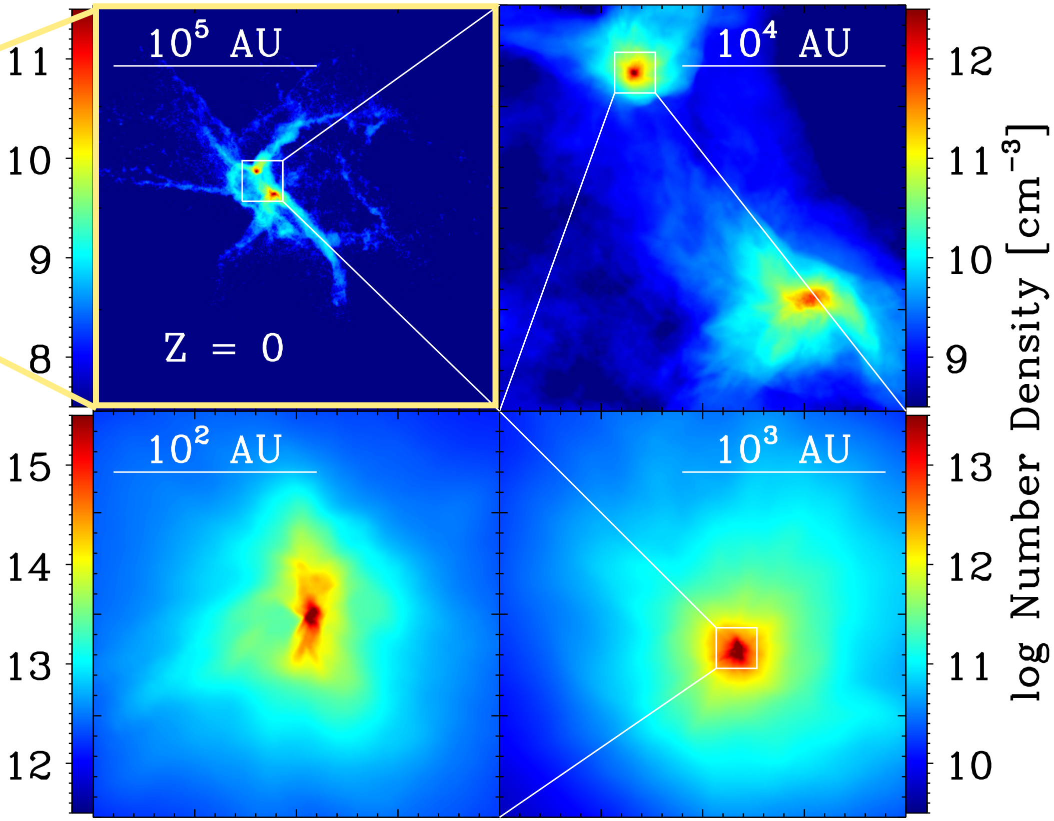

(Greif et al. 2011, Dopcke et al., in preparation)

detailed look at accretion disk around first star

successive zoom-in calculation from cosmological initial conditions (using SPH and new grid-code AREPO)

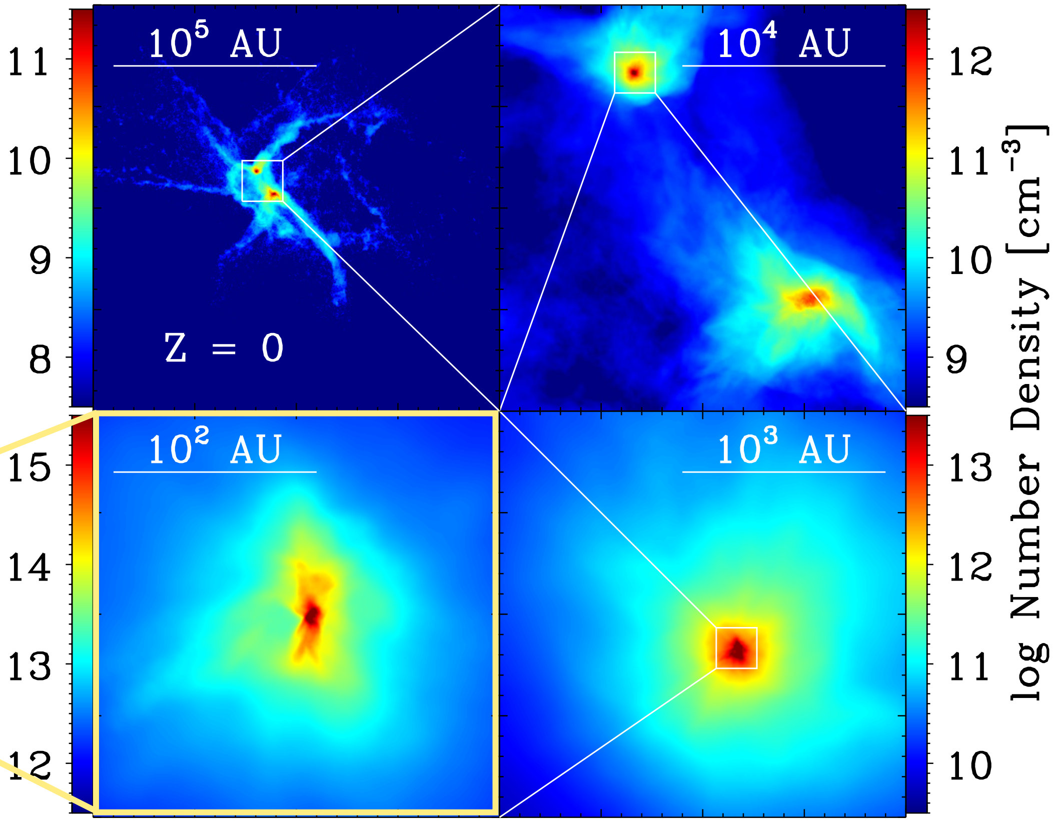

what is the time evolution of accretion disk around first star to form?

(Greif et al. 2011, Dopcke et al., in preparation) detailed look at accretion disk

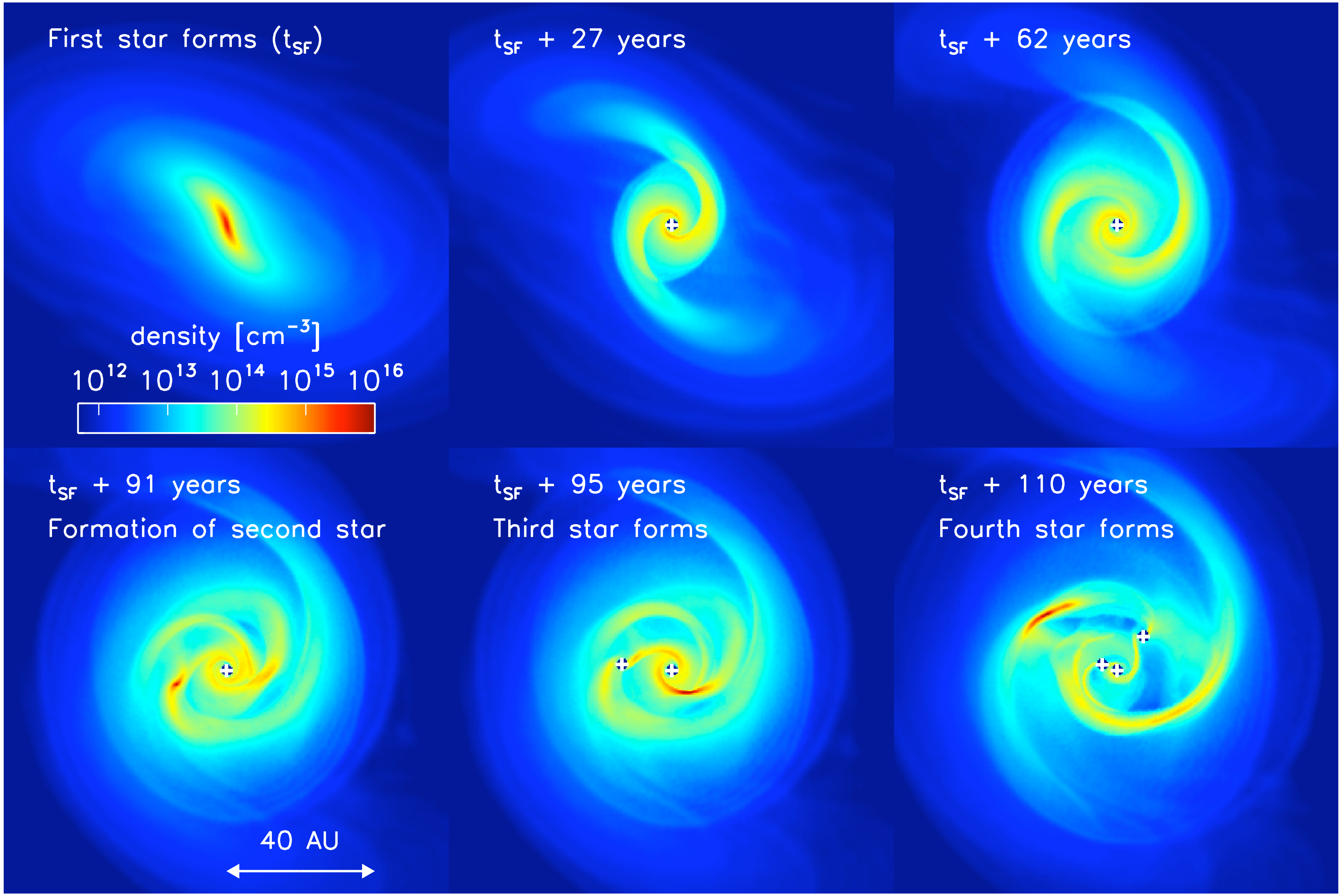

Figure 1: Density evolution in a 120 AU region around the first protostar, showing the build-up of the protostellar disk and its eventual fragmentation. We also see ‘wakes’ in the low-density regions, produced by the previous passage of the spiral arms.

(Clark et al. 2011b, Science, 331, 1040)

important disk parameters

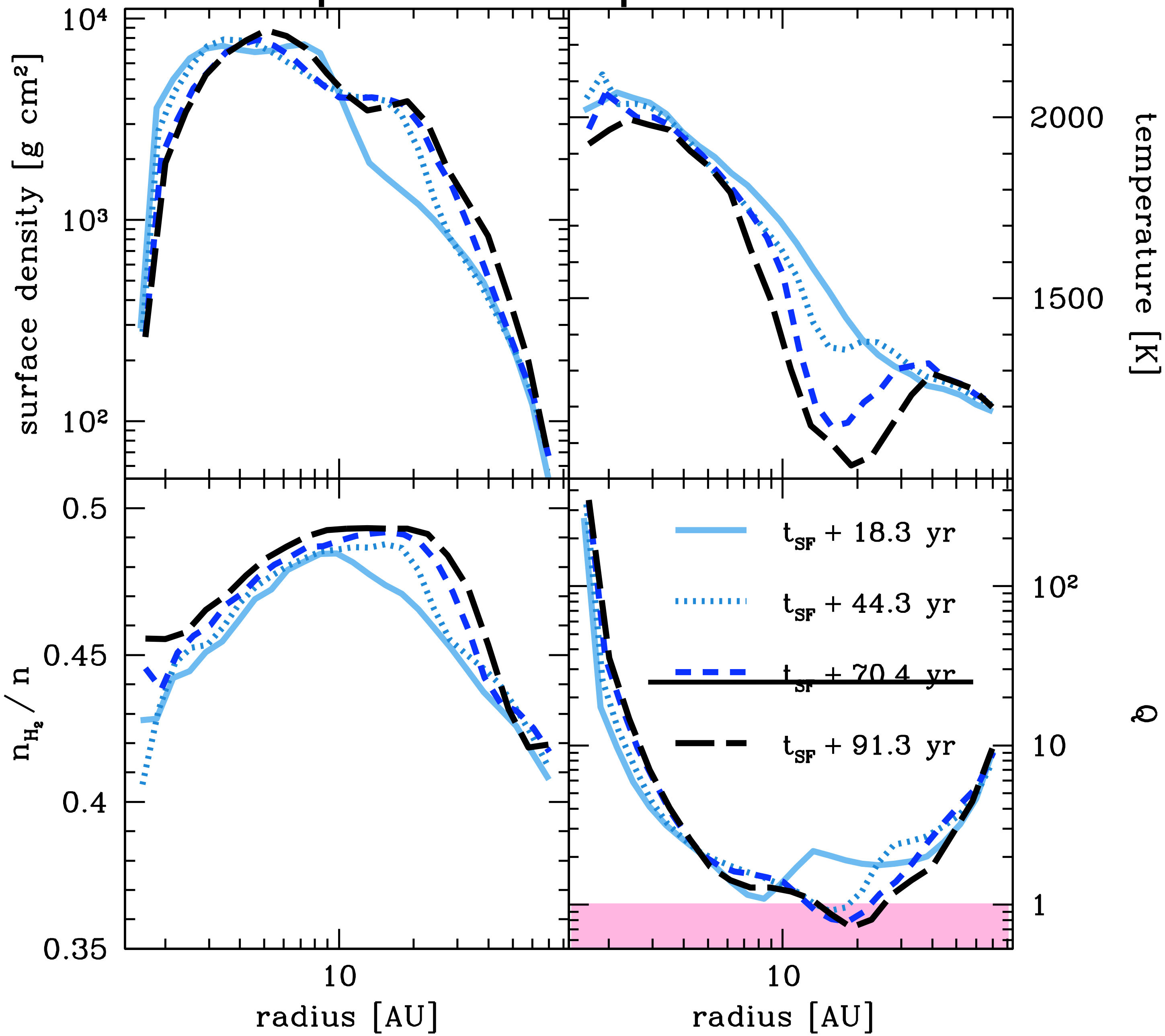

$$Q = c_{\rm s}\kappa/\pi G\Sigma$$

(Clark et al. 2011b, Science, 331, 1040)

Teaser: *fully sink-less simulations, following the disk build-up over 15 years (resolving the protostars - first cores - down to 100 km)*

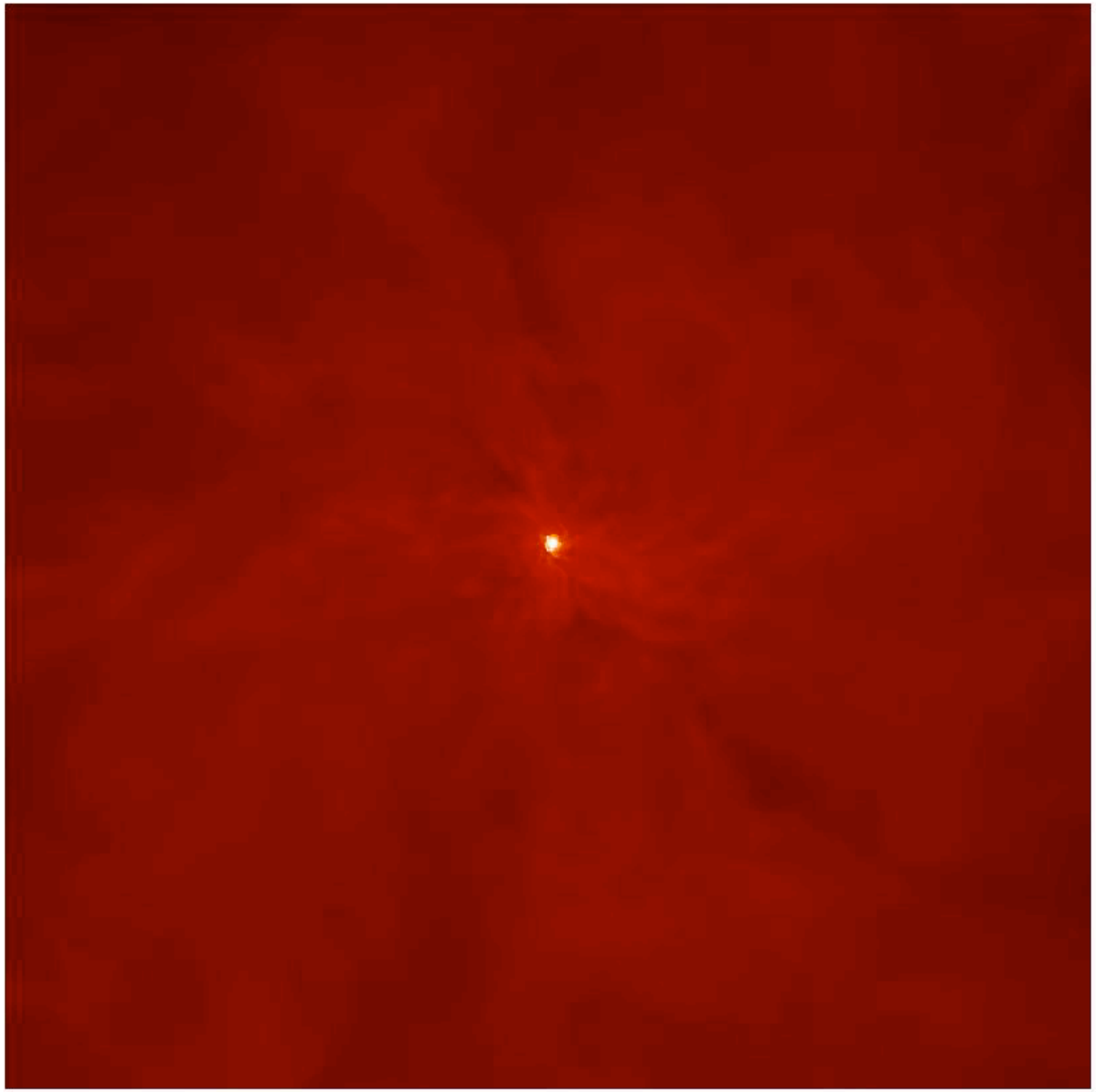

(Greif et al., in prep.)

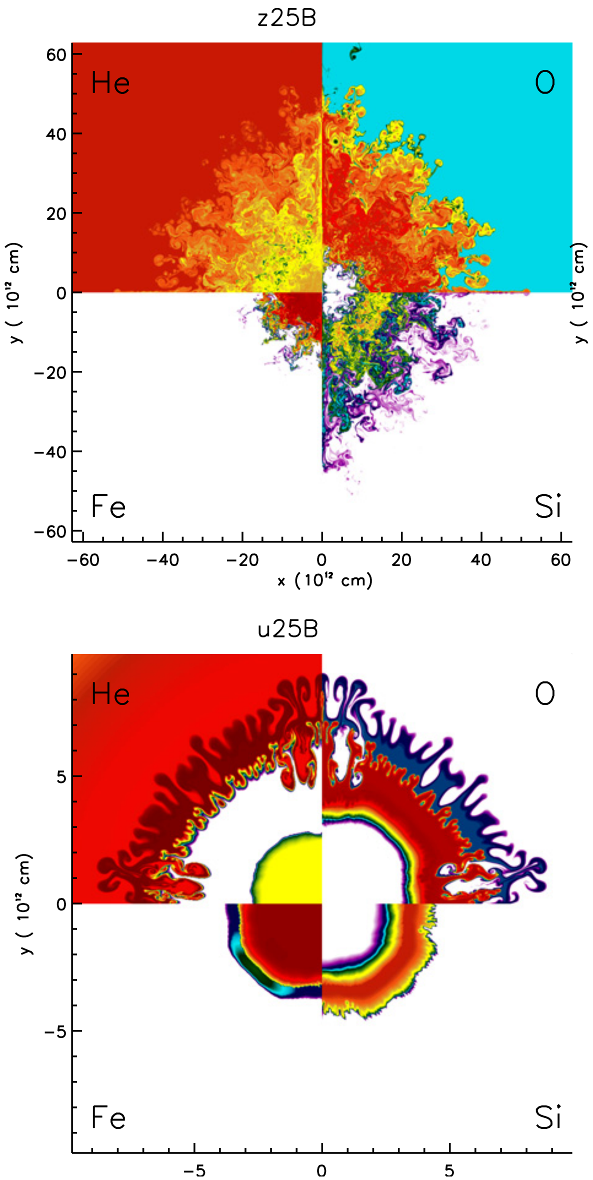

(Joggerst et al. 2009, 2010)

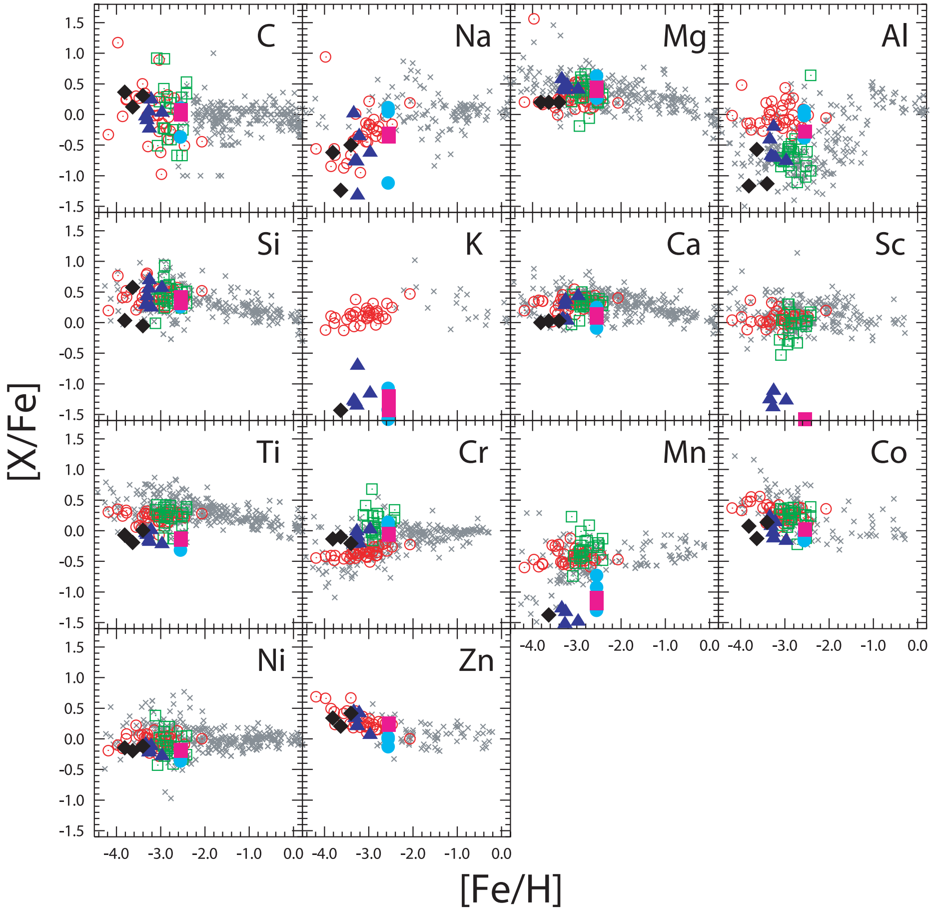

(Tominaga et al. 2007)

The metallicities of extremely metal-poor stars in the halo are consistent with the yields of core-collapse supernovae, i.e. progenitor stars with 20 - 40 M$_\odot$

(e.g. Tominaga et al. 2007, Izutani et al. 2009, Joggerst et al. 2009, 2010)

TreeCol

TreeCol

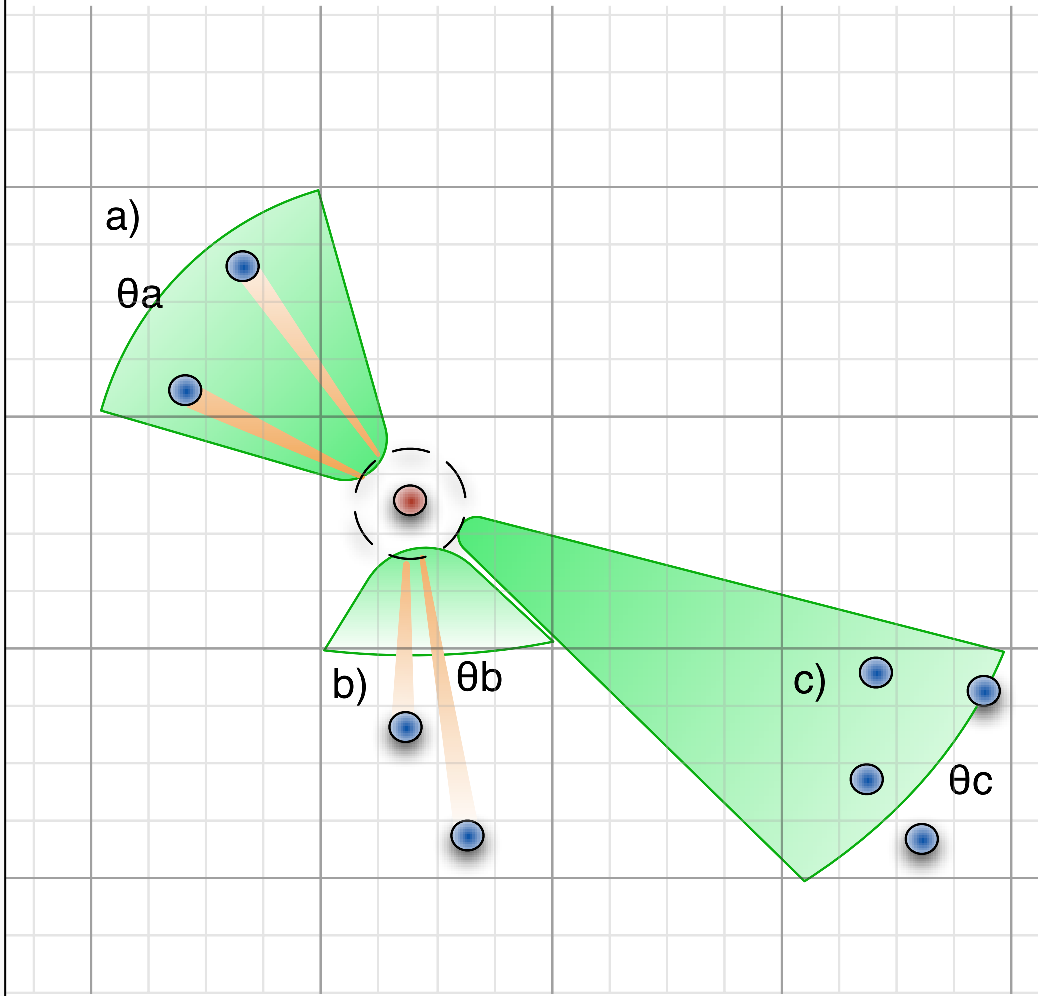

IDEA

- (gravitational) tree-walk
- calculated column densities
- accumulate on HEALPIX sphere

(Clark, Glover, Klessen, 2012, MNRAS, 420, 745)

TreeCol

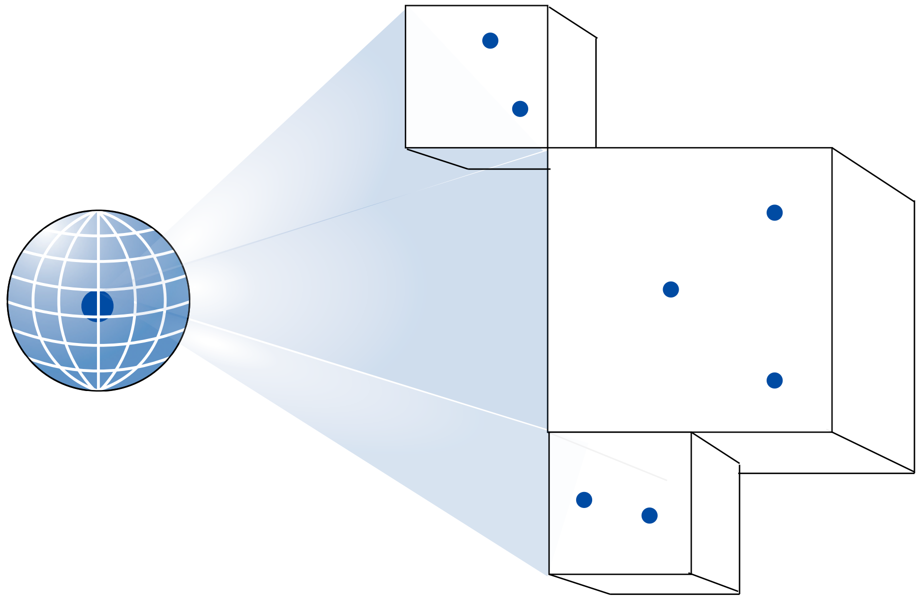

Figure 2. Schematic diagram illustrating the *TreeCol* concept. During the tree walk to obtain the gravitational forces, the projected column densities of the tree nodes (the boxes shown on the right) are mapped onto a spherical grid surrounding the particle for which the forces are being computed (the "target" particle, shown on the left). The tree already stores all of the information necessary to compute the column density of each node, the position of the node in the plane of the sky of the target particle, and the angular extent of the node. This information is used to compute the column density map at the same time that the tree is being walked to calculate the gravitational forces. Provided that the tree is already employed for the gravity calculation, the information required to create the 4π steradian map of the column densities can be obtained for minimal computational cost.

IDEA

- (gravitational) tree-walk
- calculated column densities
- accumulate on HEALPIX sphere

PERFORMANCE

- adds little computational overhead to gravitational tree-walk
- *but:* can add considerable memory overhead

(Clark, Glover, Klessen, 2012, MNRAS, 420, 745)

TreeCol

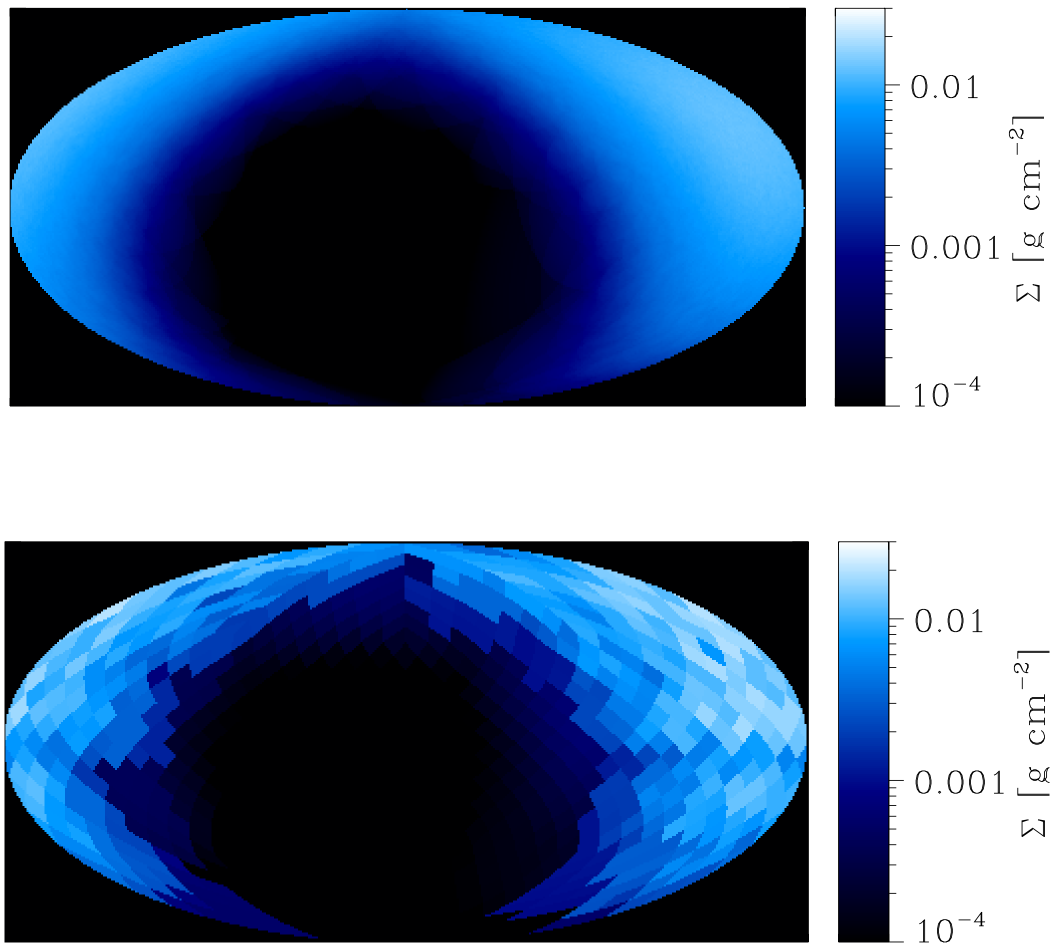

IDEA

- (gravitational) tree-walk
- calculated column densities
- accumulate on HEALPIX sphere

PERFORMANCE

- adds little computational overhead to gravitational tree-walk
- but: can add considerable memory overhead

- approximation usually good to a few percent!

(Clark, Glover, Klessen, 2012, MNRAS, 420, 745)

numerical intermezzo

TreeCol

Model	N_{pix}	θ_{tol}	$\bar{\Sigma}$ [g cm^{-2}]	Error [%]
Spherical cloud			3.060×10^{-3}	
	48	0.3	3.234×10^{-3}	5.7
	48	0.5	3.274×10^{-3}	7.0
	192	0.3	3.205×10^{-3}	4.7
	192	0.5	3.239×10^{-3}	5.8
	768	0.3	3.192×10^{-3}	4.3
	768	0.5	3.226×10^{-3}	5.4
Turbulent cloud			1.151×10^{-2}	
	48	0.3	1.126×10^{-2}	2.2
	192	0.3	1.125×10^{-2}	2.3
	768	0.3	1.133×10^{-2}	1.6

PERFORMANCE

- approximation usually good to a few percent!
- example: protostellar core, comparison with RADMC

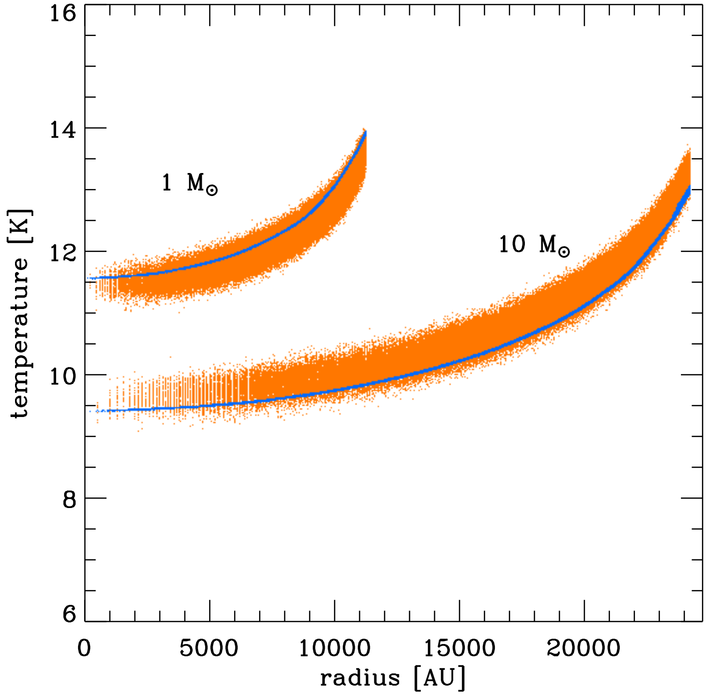

(Clark, Glover, Klessen, 2012, MNRAS, 420, 745)

B fields in the early universe?

- we know the universe is magnetized (now)
- knowledge about B-fields in the high-redshift universe is extremely uncertain
    - inflation / QCD phase transition / Biermann battery / Weibel instability
- they are thought to be extremely small
- however, *THIS MAY BE WRONG*!

small-scale turbulent dynamo

- *idea:* the small-scale turbulent dynamo can generate strong magnetic fields from very small seed fields
- *approach:* model collapse of primordial gas ---> formation of the first stars in low-mass halo at redshift z ~ 20
- *method:* solve ideal MHD equations with very high resolution
  - grid-based AMR code FLASH (effective resolution 65536^3)

questions

- *small-scale turbulent dynamo* is expected to operate during Pop III star formation
- process is *fast* ($10^4 \times t_{ff}$), so primordial halos may collapse with B-field at *saturation level!*
- simple models indicate *saturation levels of ~10%* --> larger values via $\alpha\Omega$ dynamo?
- *QUESTIONS:*
  - does this hold for "proper" halo calculations (with chemistry and cosmological context)?
  - what is the strength of the seed magnetic field?

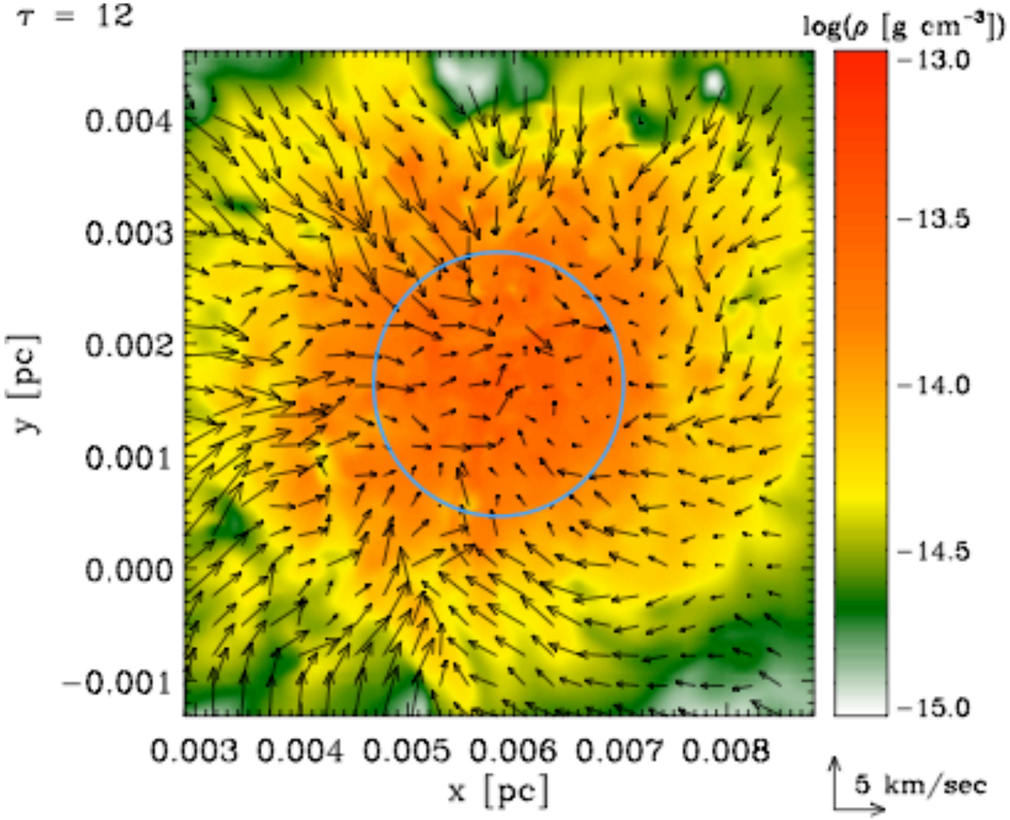

magnetic field structure

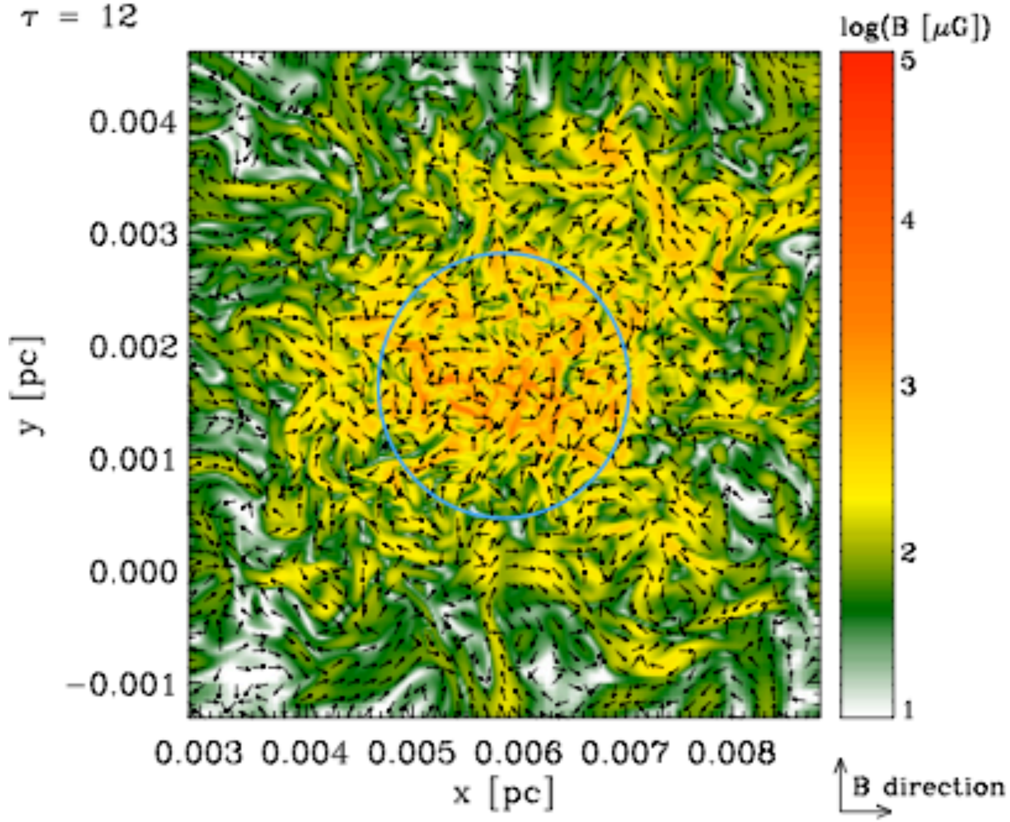

density structure

(Sur et al. 2010, ApJ, 721, L734)

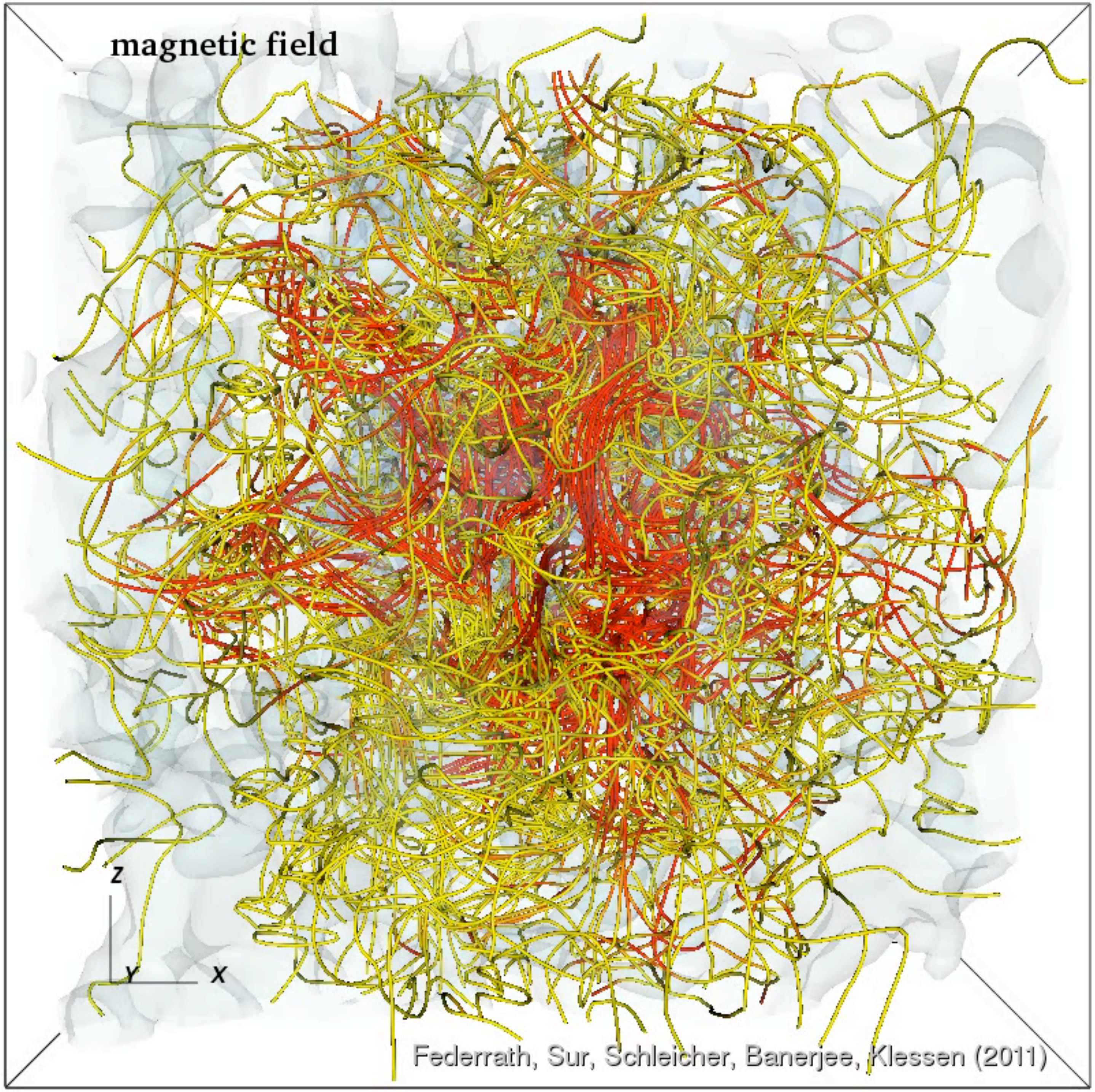

(Federrath et al., 2011, ApJ, 731, 62)

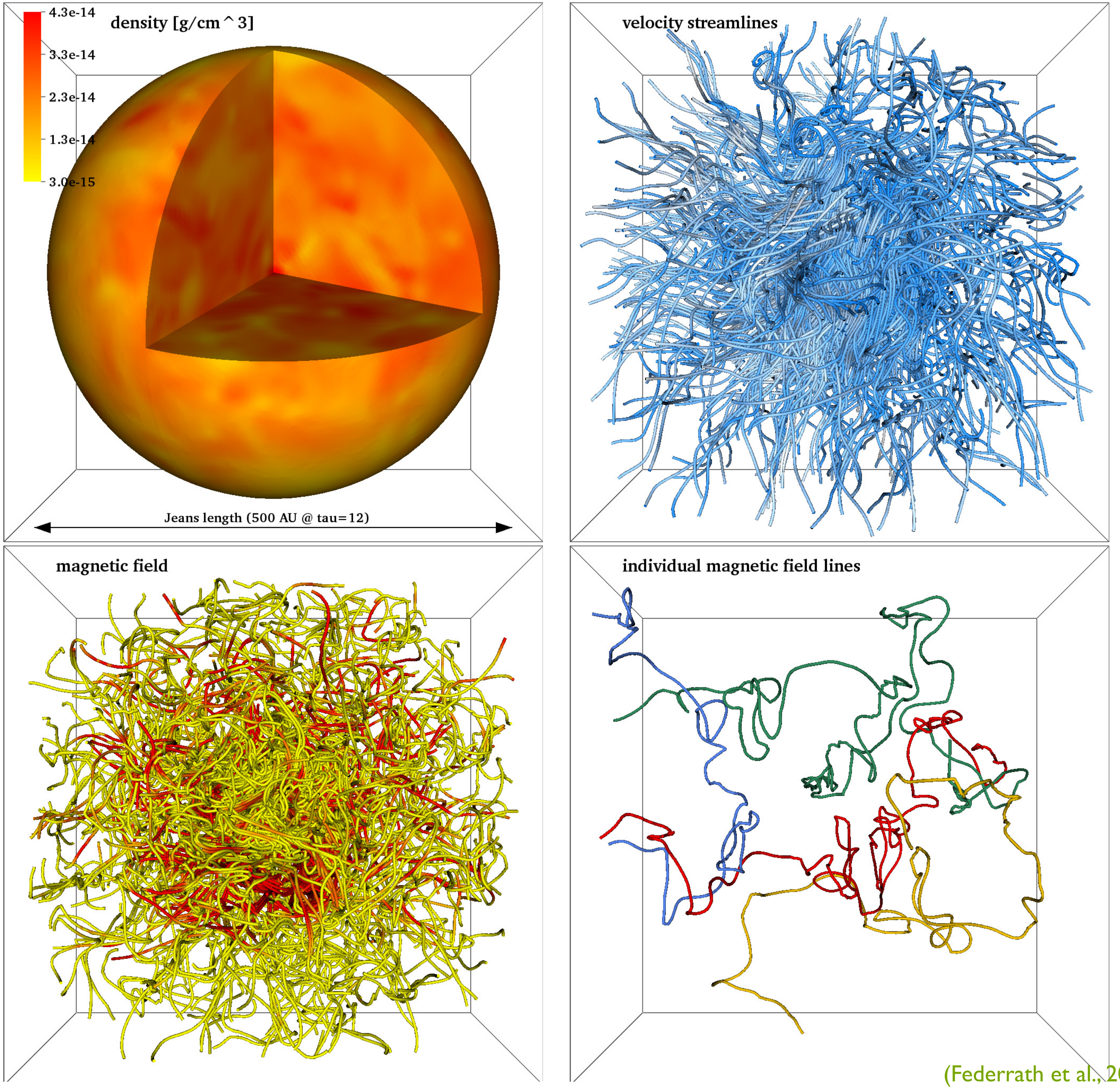

(Federrath et al., 2011, ApJ, 731, 62)

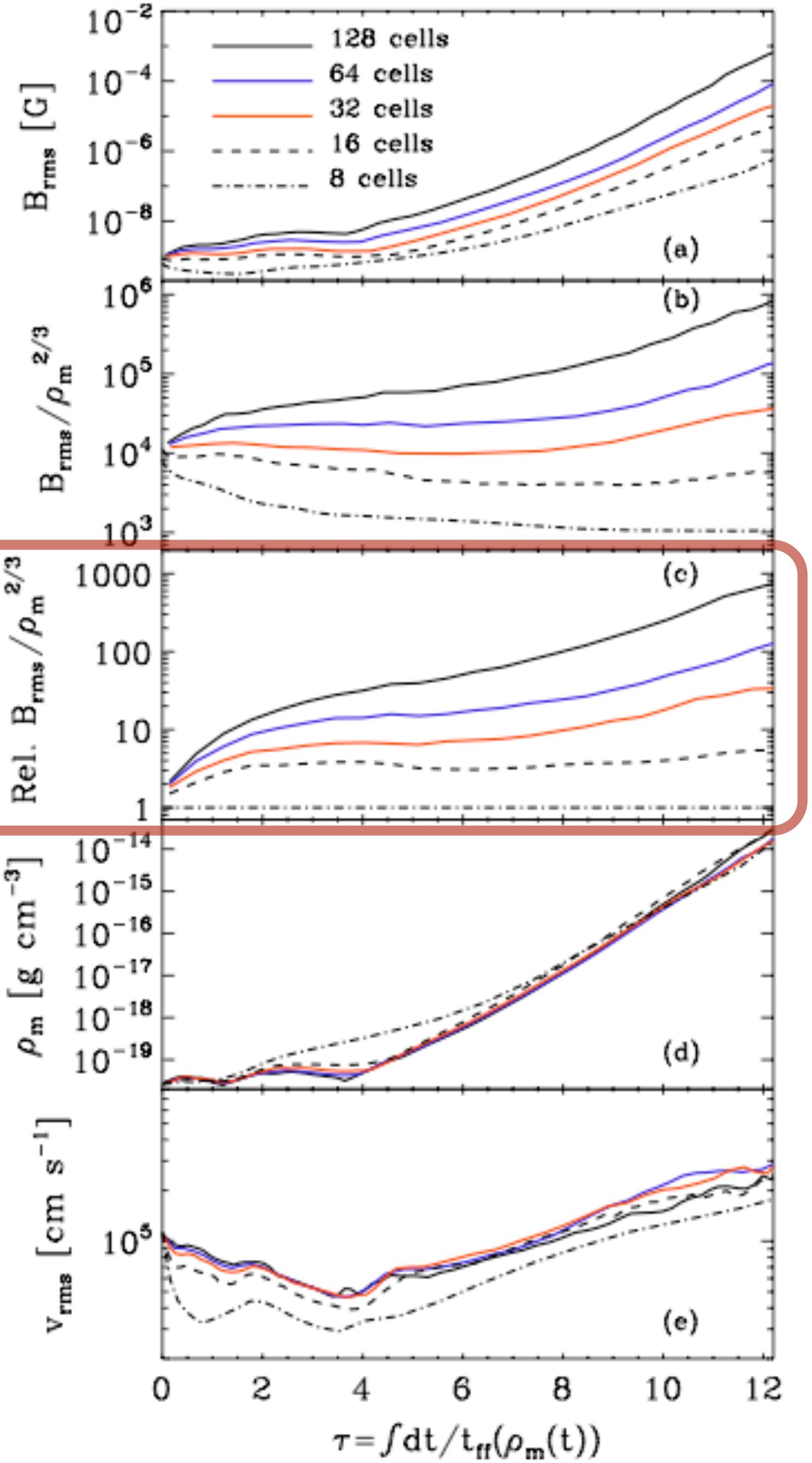

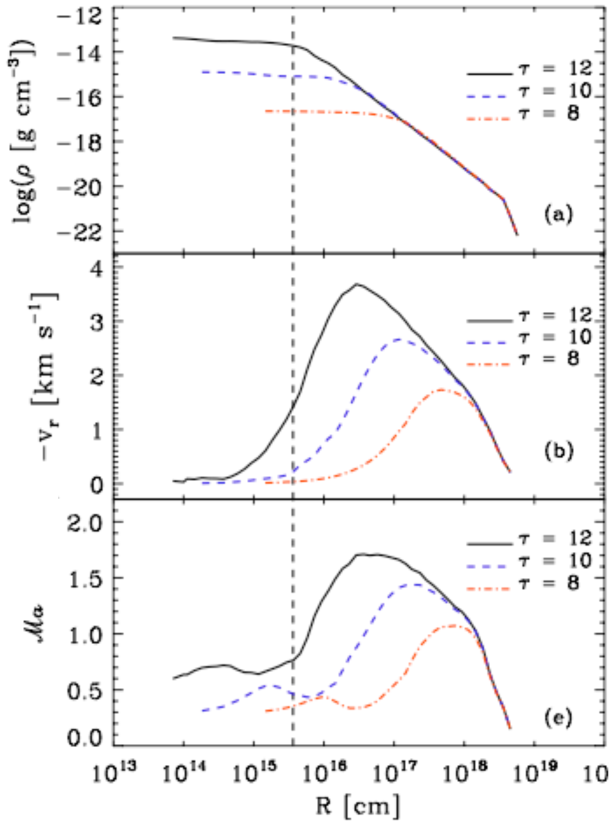

radial density profile

radial velocity profile

Mach number profile

Field amplification during first collapse seems unavoidable.

QUESTIONS:

- Is it really the small scale dynamo?
- What is the saturation value?
  Can the field reach dynamically important strength?

(Sur et al. 2010, ApJ, 721, L734)

analysis of magnetic field spectra

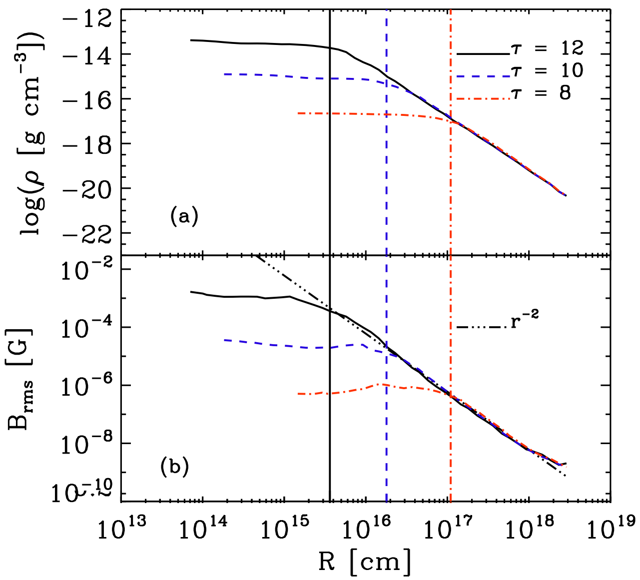

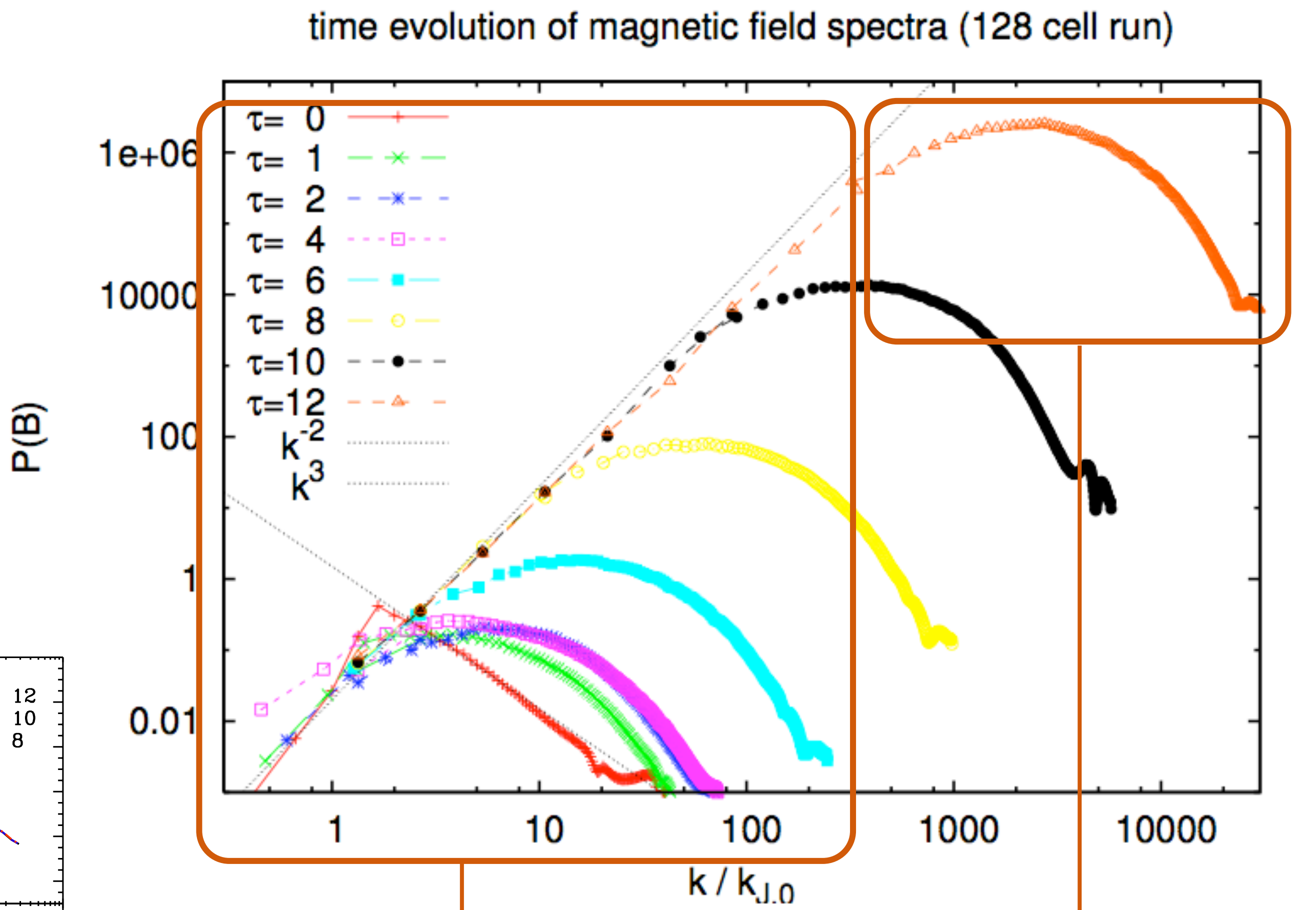

B fluctuation spectrum in $1/r^2$ fall-off

B fluctuation spectrum in flat inner core

(Federrath et al., 2011, ApJ, 731, 62)

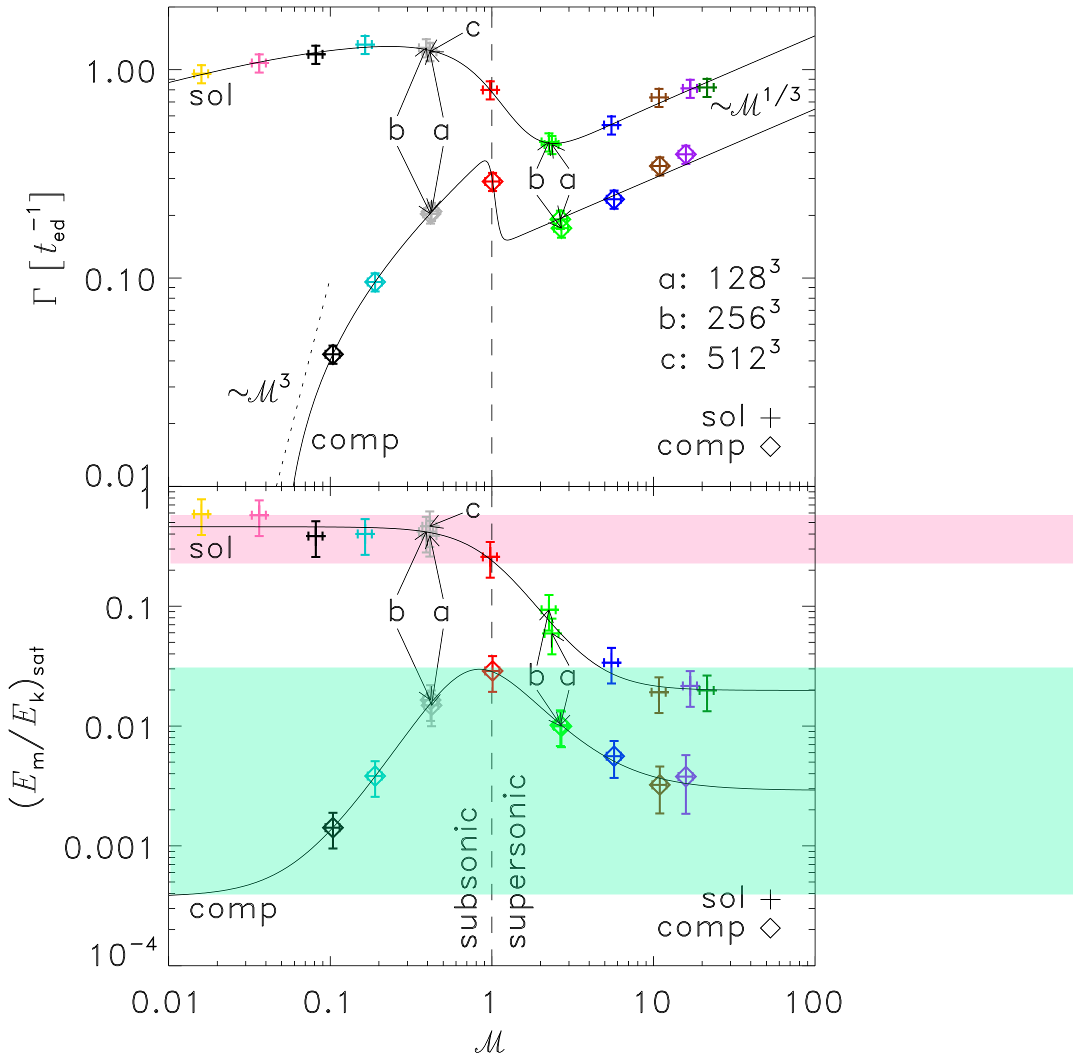

saturation level for subsonic, solenoidal turbulence

saturation level for subsonic, compressive turbulence

FIG. 3. (Color online) Growth rate (top), and saturation level (bottom) as a function of the Mach number for all runs with solenoidal (crosses) and compressive forcing (diamonds). The solid lines show empirical fits with equation (4). The labeled data points indicate four models ($\mathcal{M} \approx 0.4$, 2.5 for sol. and comp. forcing), using ideal MHD on 128^3 grid cells (a), non-ideal MHD on 256^3 (b), and 512^3 grid cells (c), demonstrating convergence for the given magnetic Prandtl (Pm = 2) and kinematic Reynolds number (Re ≈ 1500).

(Federrath et al., 2011, PRL, 107, 114505)

turbulent velocity field

separation of smooth and turbulent component:

$$\vec{v} = \vec{v}_0 + \delta \vec{v}$$

properties of turbulent field $\delta \vec{v}$:

- isotropic and homogeneous
- Gaussian random field with zero mean
- delta-correlated in time

spatial two-point correlation of fluctuations:

$$\langle \delta v^i(\vec{x}, t) \delta v^j(\vec{y}, s) \rangle = T^{ij}(r) \delta(t-s)$$

$$T^{ij}(r) = (\delta^{ij} - \frac{r^i r^j}{r^2}) T_N(r) + \frac{r^i r^j}{r^2} T_L(r)$$

(Schober et al., 2012, PRE, in press)

model for T_L

model for general turbulence:

$$T_L(r) \propto \begin{cases} \left(1 - Re^{(1-\vartheta)/(1+\vartheta)} \left(\frac{r}{L}\right)^2\right) & , r < l_c \\ \left(1 - \left(\frac{r}{L}\right)^{1+\vartheta}\right) & , l_c < r < L \\ 0 & , L < r \end{cases}$$

(l_c: cut-off scale, L: scale of largest fluctuations,
$Re = VL/\nu$: Reynolds number)

different turbulence models (in the inertial range):

$$v(l) \propto l^{\vartheta}$$

$1/3$ (Kolmogorov) $\leq \vartheta \leq 1/2$ (Burgers)

(Schober et al., 2012, PRE, in press)

MHD dynamo

idea: divide also magnetic field into mean and turbulent component

$$\vec{B} = \vec{B}_0 + \delta \vec{B}$$

put into induction equation:

$$\frac{\partial \vec{B}}{\partial t} = \nabla \times (\vec{v} \times \vec{B}) + \eta \nabla^2 \vec{B}$$

=> evolution equations for mean and turbulent field (large-scale dynamo and small-scale dynamo)

(Schober et al., 2012, PRE, in press)

Kazantsev theory

"Kazantsev Theory" (Kazantsev, 1968):
theory of the small-scale dynamo

correlation function of magnetic fluctuation:

$$\left\langle \delta B^i(\vec{x},t)\,\delta B^j(\vec{y},t)\right\rangle = M^{ij}(r,t)$$

$$M^{ij} = \left(\delta^{ij} - \frac{r^i r^j}{r^2}\right) M_N + \frac{r^i r^j}{r^2} M_L$$

with $\nabla \cdot \vec{B} = 0$:

$$M_N = \frac{1}{2\mathrm{r}} \frac{\partial}{\partial r}\left(r^2 M_L\right)$$

(Schober et al., 2012, PRE, in press)

Kazantsev theory

put magnetic correlation function into induction equation
=> Kazantsev equation:

$$M_L(r,t) \propto \Psi(r) e^{2\Gamma t}$$

$$-\kappa_T(r) \frac{\partial^2 \Psi(r)}{\partial^2 r} + U_0(r)\Psi(r) = -\Gamma \Psi(r)$$

$\kappa_T(r) = \kappa_T(T_L(r), \eta)$ "mass"

$U_0(r) = U_0(T_L(r), T_N(r), \eta)$ "potential"

can be solved with WKB-approximation for large magnetic Prandtl numbers (ν/η)

(Schober et al., 2012, PRE, in press)

critical mag. Reynolds number

Reynolds number for minimal growth rate:
set $\Gamma = 0$ in Kazantsev equation
and solve for Rm $(Rm = VL/\eta)$

result (for Kolmogorov turbulence):

$$Rm > 110$$

result (for Burgers turbulence):

$$Rm > 2700$$

=> need high resolution in order to see dynamo in simulations

(Schober et al., 2012, PRE, in press)

growth rate

growth rate for large magnetic Prandtl numbers:

$$\Gamma \propto Re^{(1-\vartheta)/(1+\vartheta)}$$

(with slope of the turbulent velocity spectrum $v(l) \propto l^{\vartheta}$)

example 1: Kolmogorov turbulence

$$\Gamma \propto Re^{1/2}$$

example 2: Burgers turbulence

$$\Gamma \propto Re^{1/3}$$

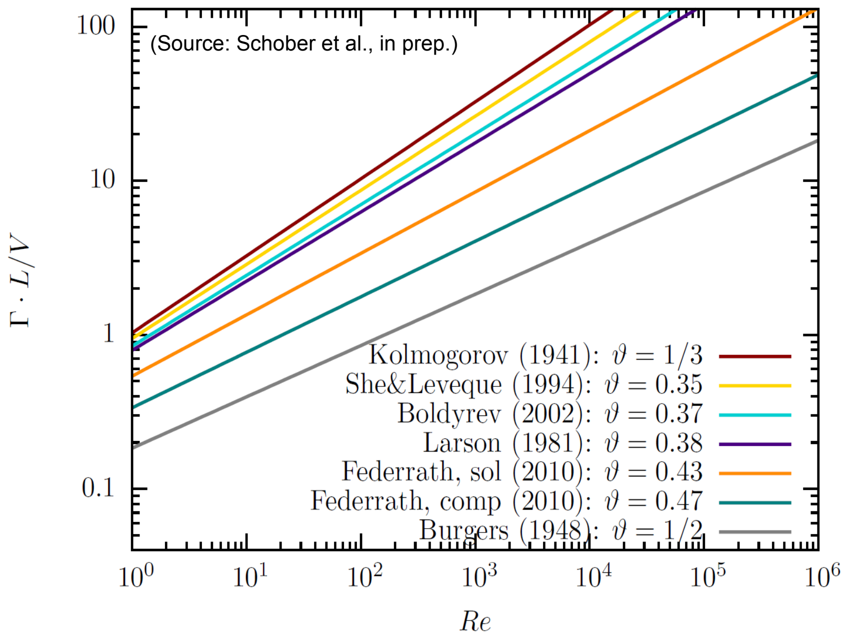

(Schober et al., 2012, PRE, in press)

dynamo in early universe

calculation of characteristic quantities in primordial gas with the chemistry code of Glover & Savin (2009)

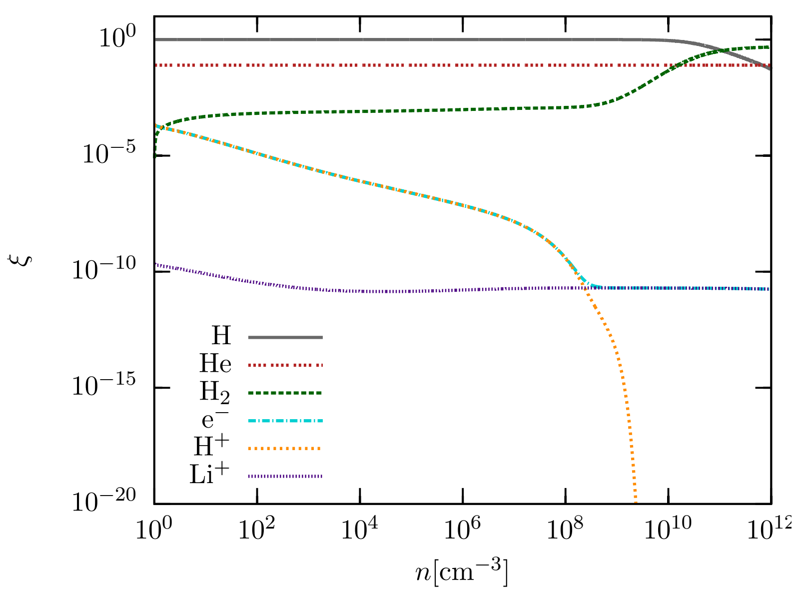

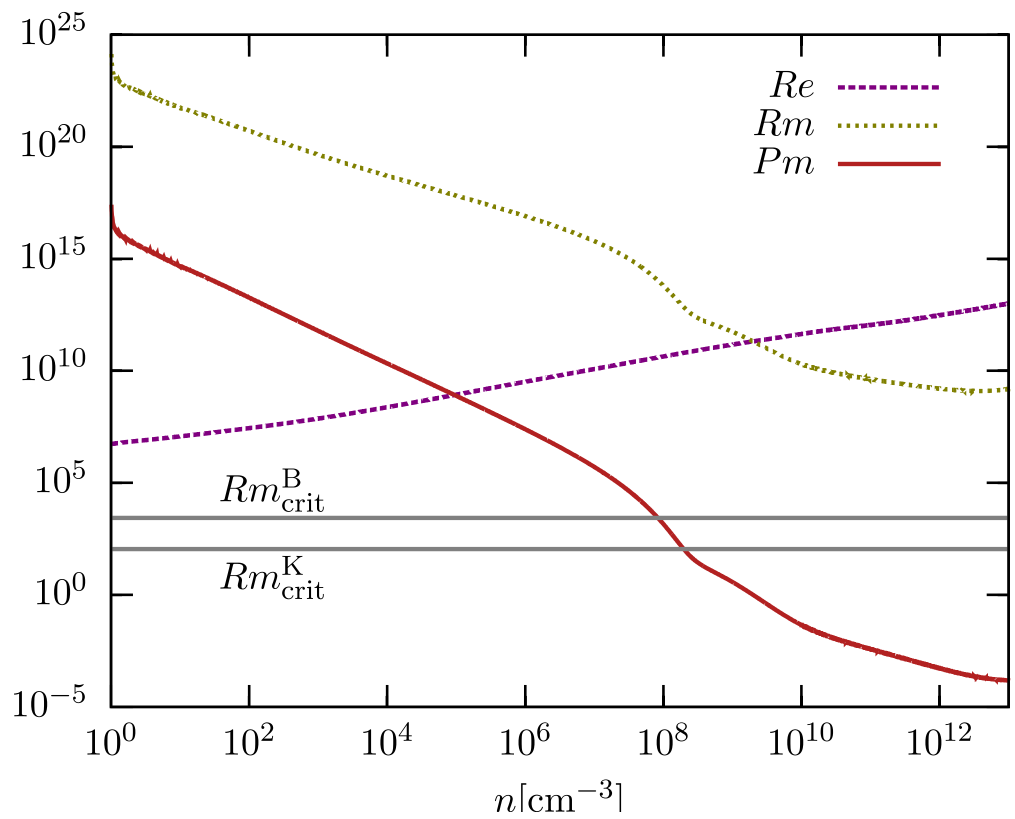

(Schober et al., 2012, PRE, in press)

in primordial minihalos

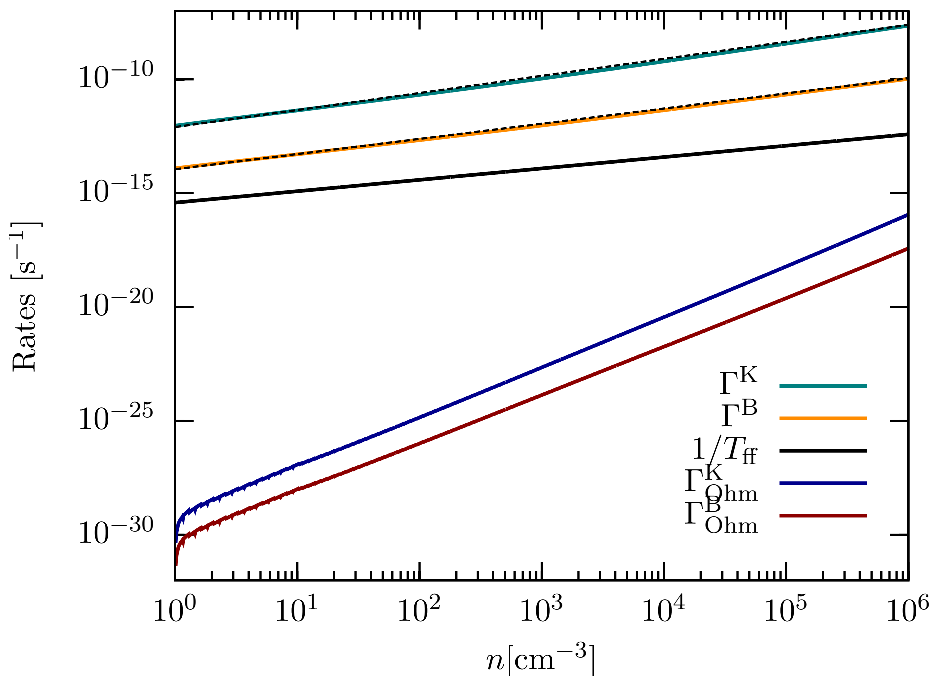

amplification vs. dissation rates

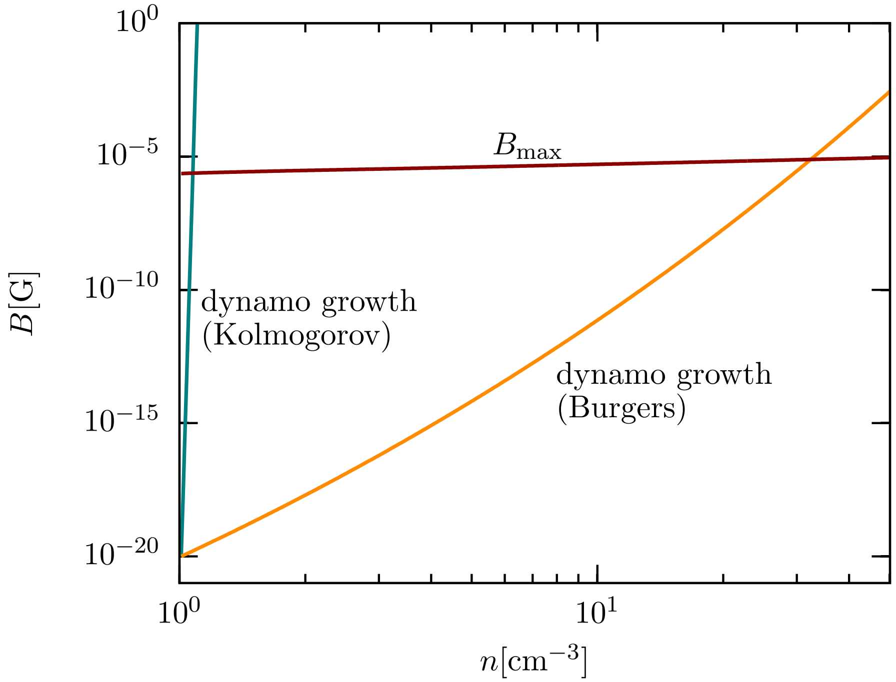

expected field strength

(Schober et al. 2012, ApJ in prep.)

questions

- *small-scale turbulent dynamo* is expected to operate during Pop III star formation
- process is *fast* (10^4 x t_{ff}), so primordial halos may collapse with B-field at *saturation level!*
- simple models indicate *saturation levels of ~10%* --> larger values via $\alpha\Omega$ dynamo?
- *QUESTIONS:*
  - does this hold for "proper" halo calculations (with chemistry and cosmological context)?
  - what is the strength of the seed magnetic field?


Carina with HST


Star formation is intrinsically a multi-scale and multi-physics problem, where it is difficult to single out individual processes.
Carina with HST

Star formation is intrinsically a multi-scale and multi-physics problem, where it is difficult to single out individual processes.

- stars form from the **complex interplay** of **self-gravity** and a large number of competing processes (such as **turbulence**, **B-field**, **feedback**, **thermal pressure**)

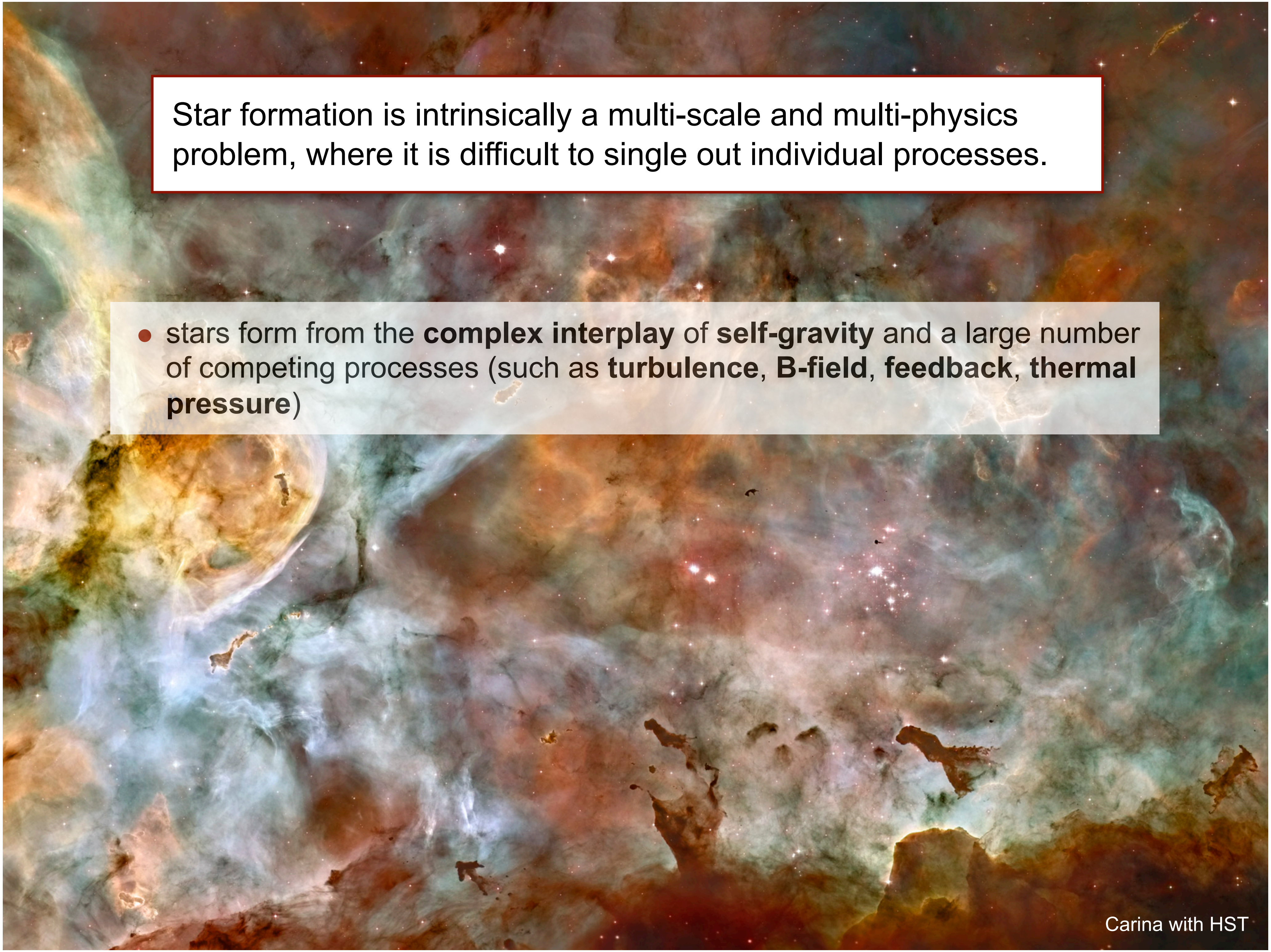

Carina with HST

Star formation is intrinsically a multi-scale and multi-physics problem, where it is difficult to single out individual processes.

- stars form from the **complex interplay** of **self-gravity** and a large number of competing processes (such as **turbulence**, **B-field**, **feedback**, **thermal pressure**)
- detailed studies require the **consistent treatment** of many **different physical processes** (this is a theoretical and computational challenge)

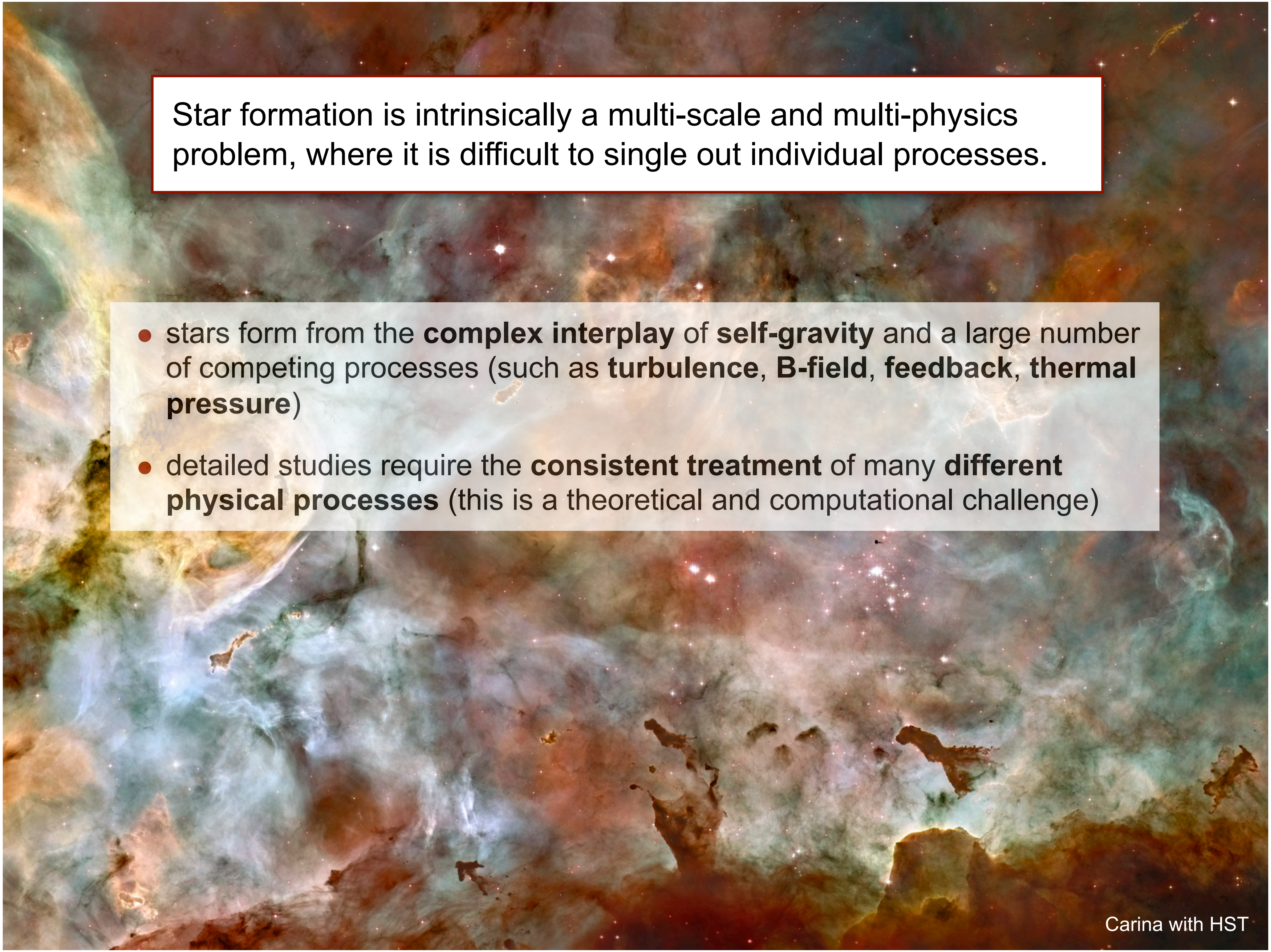

Carina with HST

Star formation is intrinsically a multi-scale and multi-physics problem, where it is difficult to single out individual processes.

- stars form from the **complex interplay** of **self-gravity** and a large number of competing processes (such as **turbulence**, **B-field**, **feedback**, **thermal pressure**)
- detailed studies require the **consistent treatment** of many **different physical processes** (this is a theoretical and computational challenge)
- star formation is **regulated** by several **feedback loops**, which are still poorly understood

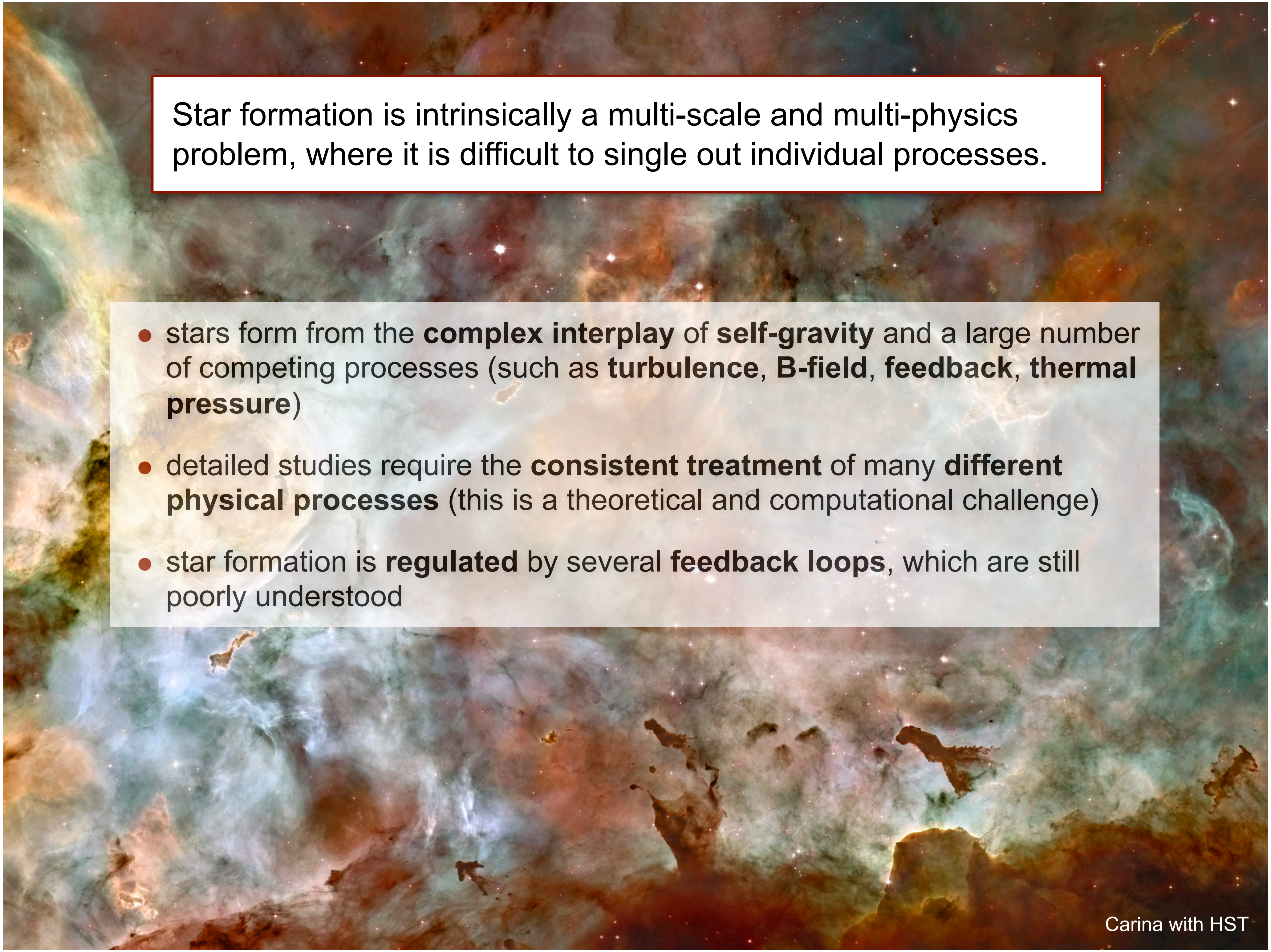
Carina with HST

Star formation is intrinsically a multi-scale and multi-physics problem, where it is difficult to single out individual processes.

- stars form from the **complex interplay** of **self-gravity** and a large number of competing processes (such as **turbulence**, **B-field**, **feedback**, **thermal pressure**)
- detailed studies require the **consistent treatment** of many **different physical processes** (this is a theoretical and computational challenge)
- star formation is **regulated** by several **feedback loops**, which are still poorly understood

progress in understanding stellar birth at present days and in the early universe depends on developing new multi-scale and multi-physics numerical methods

Carina with HST


PPVI comes to Heidelberg
in summer 2013


PPVI comes to Heidelberg
in summer 2013
... hope to see you there!!!